Feasibility Study of the Use of the Acoustic Velocity Meter for Measurement of Net Outflow From the Sacramento–San Joaquin Delta in California

---

GEOLOGICAL SURVEY WATER-SUPPLY PAPER 1877

Prepared in cooperation with the California Department of Water Resources and U.S. Army Corps of Engineers

Feasibility Study of the Use of the Acoustic Velocity Meter for Measurement of Net Outflow From the Sacramento–San Joaquin Delta in California

By WINCHELL SMITH

GEOLOGICAL SURVEY WATER-SUPPLY PAPER 1877

Prepared in cooperation with the California Department of Water Resources and U.S. Army Corps of Engineers

UNITED STATES GOVERNMENT PRINTING OFFICE, WASHINGTON : 1969

UNITED STATES DEPARTMENT OF THE INTERIOR

WALTER J. HICKEL, *Secretary*

GEOLOGICAL SURVEY

William T. Pecora, *Director*

Library of Congress catalog-card No. 71-650227

For sale by the Superintendent of Documents, U.S. Government Printing Office
Washington, D.C. 20402 - Price 40 cents (paper cover)

CONTENTS

ILLUSTRATIONS

TABLES

SYMBOLS

A Total area in a cross section normal to streamlines of flow.
A_p Total area in a cross section parallel to an acoustic path.
a Subsection area.
B Width of a cross section or length of an acoustic path.
b Incremental length or subsection width.
C Ratio of mean velocity in the cross section to a mean line velocity.
$\overline{C}$ Arithmetic mean value of C.
c Propagation rate of sound in still water.
d Depth of water in a vertical.
E Selected line elevation.
ϵ_A Systematic error in measured or computed discharge.
ϵ_N Random error.
H Stage or elevation of water surface above an arbitrary datum.
K A parameter equal to $C \tan \theta$
k Constant in the power-law equation.
m Exponent in the power-law equation.
N Number of hours or data sets recorded in a given computation period.
Q Computed total discharge in a stream.
Q' Actual total discharge in a stream.
Q_a Total measured discharge with systematic error due to area.
Q_c Computed discharge.
Q_M Measured discharge.
Q_N Total measured discharge with error due to number of subsections.
$\overline{Q}_n$ Average net outflow to the ocean.
Q_q Total measured discharge with error due to error in subsection discharge.
$Q_{0.2}$ Discharge computed on basis of velocity observations made at a point 0.2 of the depth below the water surface.
q Subsection discharge.
q_a Measured subsection discharge with random error due to area.
q_b Measured subsection discharge with error due to boat velocity.
q_l Measured subsection discharge with error due to horizontal angle.
q_p Measured subsection discharge with error due to boat position.
q_s Measured subsection discharge with error due to vertical velocity curve.
q_t Measured subsection discharge with error due to velocity pulsation.
q_{vb} Measured subsection discharge with error due to vertical movement of boat.
$q_{0.2}$ Subsection discharge computed from a velocity observation made at a point 0.2 of the depth below the water surface.
R_a Systematic error ratio for total discharge due to area.
R_{CM} Random error ratio due to errors in current-meter calibration.

R_M Random error ratio in computed total discharge.
R_N Random error ratio for total discharge due to number of subsections.
R_q Random error ratio for total discharge due to error in subsection discharge.
r Partial error ratio in a subsection.
r_a Random subsection error ratio due to area.
r_b Subsection error ratio due to boat velocity.
r_l Subsection error ratio due to horizontal angle.
r_p Subsection error ratio due to boat position.
r_q Combined subsection discharge error ratio.
r_s Subsection error ratio due to shape of vertical velocity curve.
r_t Subsection error ratio due to velocity pulsation.
r_{vb} Subsection error due to vertical movement of boat.
S Standard deviation of a parameter. Subscripts indicate particular parameter.
s Stationing of verticals within a cross section.
T Traveltime. Subscripts denote source and direction.
T' A recorded traveltime. Subscripts denote source and direction.
ΔT Increment between actual traveltime and recorded traveltime.
$\overline{V}$ Average velocity in a cross section normal to streamlines of flow.
V_E Average velocity along a line at an elevation E in the cross section.
V_f The friction velocity or shear velocity at the boundary.
V_n Velocity component normal to an acoustic path.
$\overline{V}_{0.2}$ Weighted average of velocities observed at points 0.2 of the depth below the water surface.
$\overline{V}_{0.8}$ Weighted average of velocities observed at points 0.8 of the depth below the water surface.
v Velocity at a point.
$\bar{v}$ Mean velocity in a vertical.
v_b Boat velocity over the bottom.
v'_b Boat velocity relative to the water.
v_y Point velocity at a distance y above the bottom of the stream.
$v_{0.2}$ Point velocity at a distance of 0.2 of the depth below the water surface.
$v_{0.8}$ Point velocity at a distance of 0.8 of the depth below the water surface.
y Distance from bottom of the stream to a point of measured or computed velocity.
Y_o A constant related to V_f and the kinematic viscosity of the fluid.
θ Angle of departure between an acoustic path and the streamline of flow.
ϕ Error between actual and assumed angles of departure.

FEASIBILITY STUDY OF THE USE OF THE ACOUSTIC VELOCITY METER FOR MEASUREMENT OF NET OUTFLOW FROM THE SACRAMENTO–SAN JOAQUIN DELTA IN CALIFORNIA

By WINCHELL SMITH

ABSTRACT

A reliable measure of the fresh-water outflow from the Sacramento–San Joaquin delta is needed for the operation of the California Water Project and for the evaluation of the interrelated water problems of the delta and San Francisco Bay regions. The Chipps Island channel, immediately downstream from the confluence of the Sacramento and San Joaquin Rivers, is the most promising site for this flow measurement, but the conventional techniques used for evaluating steady flows cannot be employed there because the channel reach is in the tidal zone, and reversals of flow occur during each tidal cycle. Net outflows, which may be as little as 2,000 cubic feet per second must necessarily be computed as the difference between the large ebbflow and floodflow volumes that move back and forth between the delta region and San Francisco Bay. Discharges during peak periods of the ebb and flood tidal cycles may exceed 300,000 cubic feet per second. In consequence, a very high degree of precision must be maintained in the gross flow measurements if meaningful computations of net outflow are to be made.

This report evaluates the probable accuracies that might be achieved by use of an AVM (acoustic velocity meter), a device which measures the stream velocity along a diagonal line across the channel. The study indicates that this line velocity will provide a stable index of the mean velocity in the channel and that such an index could be used as a primary parameter for the computation of discharge. Therefore, net outflows probably could be computed with the required accuracy by the use of such a device. The significant factors controlling the precision of measurement would be the stability of the channel geometry and streamline orientation, the precision with which the current-meter measurements needed for calibration of the system could be made, the instrumental calibration stability of the AVM system, and the length of period over which net outflows were computed.

The AVM system developed by the U. S. Geological Survey in cooperation with the California Department of Water Resources and the U. S. Army Corps of Engineers does not have the required instrumental stability for this precise flow measurement. However, other AVM systems now being produced commercially seem to have the desired error characteristics, and a system probably can be procured that will permit computation of the fresh-water outflow from the delta area.

INTRODUCTION

The Sacramento and San Joaquin Rivers drain the Central Valley of California, a watershed of approximately 43,000 square miles. These streams enter the area known as the Sacramento–San Joaquin

delta between the cities of Sacramento and Tracy. The water then disperses in a maze of channels interlacing the many islands in the delta and finally converges in an outlet channel, generally referred to as the Chipps Island channel (figs. 1 and 2), on the west side of the delta near Pittsburg. The delta covers an area of about 400,000 acres and includes more than 50 islands, most of which lie between elevations of 5 feet above mean sea level and 18 feet below mean sea level. These lands are composed of sedimentary and peat soils and are intensively farmed.

Water released from Oroville Reservoir on the Feather River, a tributary of the Sacramento River, and from Shasta Lake, on the upper Sacramento River, must be transported across the delta to pumping plants on the southwest side. Present releases from Shasta Lake are carried in the delta channels; projected releases from Oroville Reservoir probably will be carried in a peripheral canal. How-

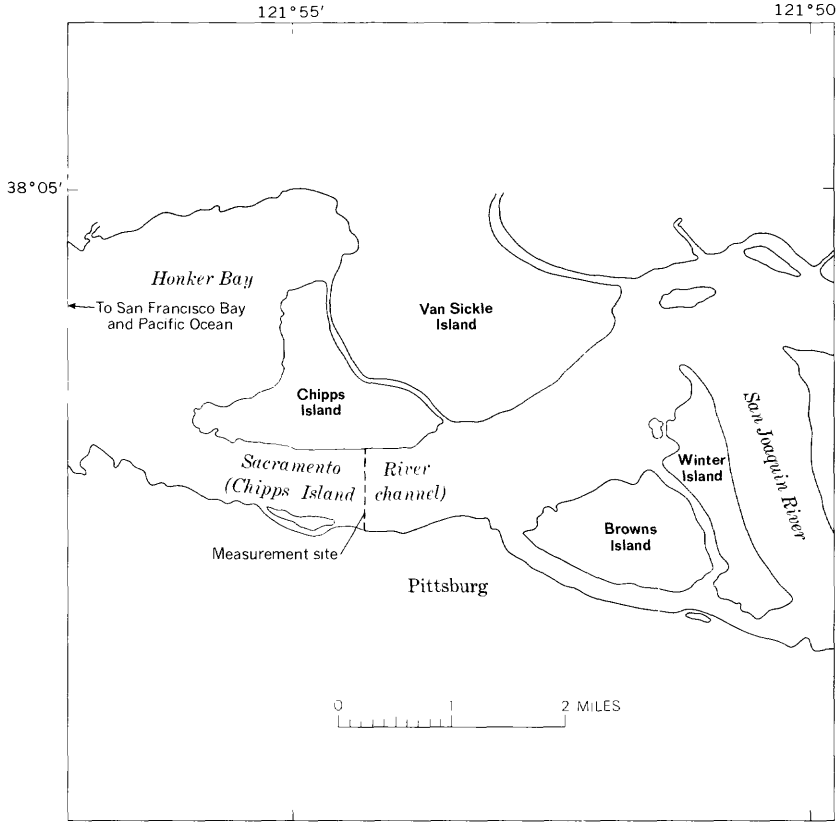

FIGURE 1.—Chipps Island area.

FIGURE 2.—Chipps Island channel. View is eastward.

ever, the quality and distribution of flows in the delta channels arer and will continue to be, directly related to the operation of the wate, projects. A significant fresh-water outflow must be maintained to control the extent of salt-water intrusion, and an objective method of measuring this outflow is needed.

The 2½-mile-long channel opposite Chipps Island is affected by tidal action, and reversals of flow occur during each of the twice-daily tidal cycles. Gross flows that exceed 300,000 cfs (cubic feet per second) may occur during peaks of each ebb and flood period. The average daily fresh-water outflow may be as little as 2,000 cfs. Conventional stream-gaging techniques cannot be used under such conditions, but two specialized techniques seem to hold promise. These are the application of the analytical procedure developed by Baltzer and Shen (1961, p. C39) and the use of an acoustic-velocity-measuring system. Proper evaluation of the Baltzer-Shen analytical method will require installation of structures in the channel; but, because a cursory study of the problems associated with the use of this method in the

334-224 O—69——2

short Chipps Island channel casts considerable doubt on the probabilities for success, the primary focus of this report is centered on evaluation of the acoustic-velocity-metering system.

The AVM (acoustic velocity meter) is a device which measures the average water velocity along a horizontal line oriented diagonally to the streamlines of flow. This is done by timing the rate of travel of acoustic signals transmitted in both directions along the path. Experience to date (June 1966) indicates that in stable flow regimes such a line velocity is a valid index of the mean velocity in the cross section.

PURPOSE AND SCOPE

Evaluation of the fresh-water outflow from the delta depends upon computation of the difference between the ebb and flood flows in the tidal reach. This difference is a small fraction of the total flow involved, and, in consequence, extremely high accuracies must be maintained in measurement of the actual flows. The purpose of this study is to evaluate the probable accuracies that can be attained so that a decision as to feasibility of the use of an AVM can be made. The scope of the study includes the analysis of velocity profiles in the channel to evaluate the probable accuracy of the relation between the integrated line velocities which can be measured by the AVM and the mean velocity in the total cross section. The study also includes an evaluation of probable computation results as influenced by the hydraulic relations, the system errors, and calibration techniques which will, of necessity, be based on current-meter measurements in the channel.

ACKNOWLEDGMENTS

This report was prepared by the U.S. Geological Survey, in cooperation with the California Department of Water Resources and the U.S. Army Corps of Engineers. The investigation was begun under the direction of Walter Hofmann and completed under the direction of R. Stanley Lord, successive district chiefs, Water Resources Division, U.S. Geological Survey, Menlo Park, Calif. Base data used in the analysis were obtained from reports furnished by the California Department of Water Resources.

The energetic assistance furnished by E. D. Cobb and R. L. Hanson, in the early phases of the study is gratefully acknowledged, as are the contributions made by R. W. Cruff, J. R. Beck, and Reuben Lee, who participated in the field-test programs in the Sacramento River channel at Chipps Island. All are U.S. Geological Survey personnel.

THE STREAM-GAGING PROBLEM

METHODS OF DETERMINING DISCHARGE

One of the most difficult problems in hydrography is the gaging of estuarine flow. No simple stage-discharge relation exists. Peak ebb and flood discharges correspond to maximum slopes of water surface, but these peak discharges are not in precise phase with extremes of stage, as is shown in figure 3, which illustrates the variation of flow and stage in the Chipps Island channel during a typical tidal cycle. Methods suitable for solution of this gaging problem rest upon an

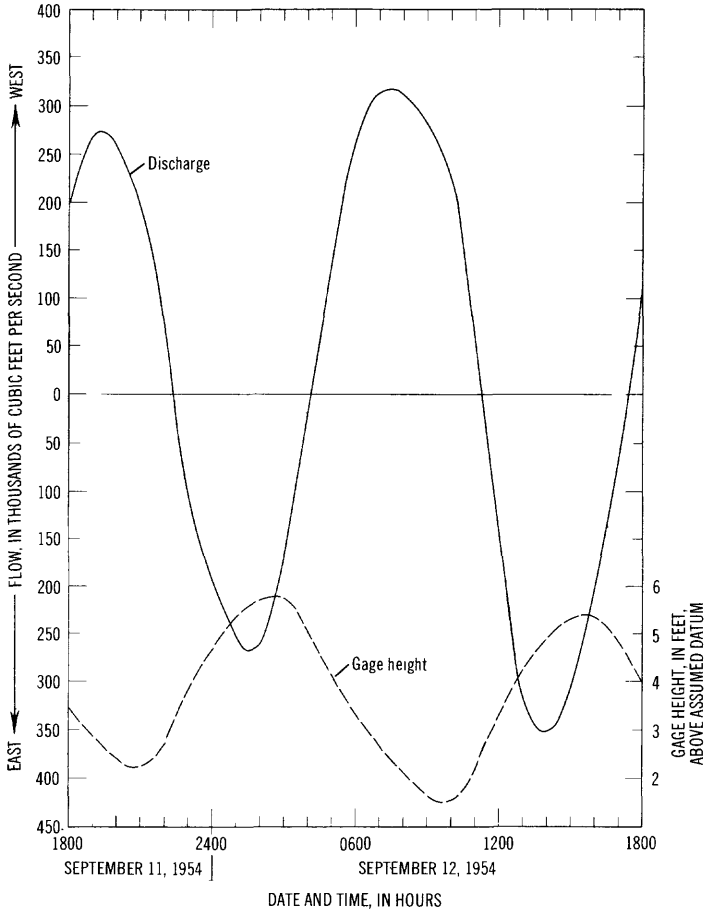

FIGURE 3.—Typical hydrographs of discharge and stage in the Sacramento River at Chipps Island.

analytical solution of the unsteady-flow equations, a direct measurement of the velocity in the channel, or the measurement of a valid index of the velocity.

The method proposed by Baltzer and Shen (1961, p. C39) for analytical solution requires simultaneous recording of water stages at the two ends of a reach that is long enough to permit accurate determination of the water-surface slope. The confined reach at Chipps Island is about 2½ miles long and half a mile wide. Rough computations indicate that the difference between water-surface elevations at the two ends of the reach would be less than 0.4 foot for more than 50 percent of the time during each tidal cycle, and, as the reach is subject to high winds and considerable wave action, stage records of the precision required for accurate flow computation probably could not be obtained. The emphasis of this report has accordingly been placed on evaluation of alternative techniques. It should be emphasized, however, that this represents only a cursory evaluation of the potentialities of the analytical technique; further study of this tool should be made as a part of any future discharge-measuring program.

A direct measurement of velocities in the channel was undertaken by the California Department of Water Resources in 1963 and 1964. A system of Savonius current meters was installed at 16 verticals in the cross section. These were connected to a remote readout console to provide continuous monitoring of velocities in the channel. This system was straightforward in its approach and had the capability of producing an accurate flow record, but it proved to be too expensive for continuous operation.

Review of literature discussing the use of velocity observations at a single point in the cross section as a velocity index (Craig, 1963; Miller, 1962) indicated that accuracies inherent in this technique are not good enough to permit evaluation of the net outflow. Thus, the concept of using a line velocity, the average velocity along a horizontal line across the major part of the channel, as an index to the mean velocity in the cross section seems to be the most practicable measuring technique available. Experience with acoustic velocity meters at test sites on the Snake River near Clarkston, Wash., and on the Delta-Mendota Canal near Tracy, Calif., has shown that a line velocity is a valid index of the mean velocity for steady-flow regimes. The analysis which follows was made to determine whether a consistent relation could be established in this tide-affected reach of channel between a line velocity at a given elevation and the mean velocity in the cross section, and to determine the probable accuracies of flow computations based on such an index.

DATA AVAILABLE FOR ANALYSIS

Considerable effort has been made in prior years to determine flow conditions, salinity gradients, and velocity distribution in the Chipps Island channel. The most comprehensive and detailed work was that reported by the Water Project Authority of the State of California (1955). This report included detailed velocity and discharge data and salinity and temperature data for the period September 11–27, 1954. Measurements were made by the moving-boat method described in the section "Accuracy of current-meter measurements" of the present report. Supplementary data included a series of multiple-point velocity observations made from anchored boats. The analysis which follows is based entirely on data from this measurement program. Data available from other sources adds very little information pertinent to the gaging problem under study.

LINE VELOCITY AS AN INDEX OF DISCHARGE

COMPUTATION OF AVERAGE LINE VELOCITY FROM CURRENT-METER MEASUREMENT DATA

The technique employed in the continuous 1954 moving-boat measurement resulted in definition of velocities at points 0.2 and 0.8 of the depth below the water surface ($v_{0.2}$ and $v_{0.8}$) at intervals of about 1 hour; observations in adjacent sections were made in sequence. To compute instantaneous discharges, the velocity observations at each section were plotted against time, and concurrent velocities were then abstracted from these curves at hourly intervals. Data available covered the 17-day period September 11–27, 1954; data for September 12–16 were plotted and used initially, and results from the analysis of those 5 days were then applied to the period September 20–24 for comparison.

Flows in a westerly direction (ebbtide) were considered positive, and those in an easterly direction (floodtide) were considered negative.

The analysis involved computation of theoretical average line velocities at selected elevations (V_E) from the data defined by the current-meter measurements. The ratios of these computed average line velocities to the concurrent mean velocities in the total cross section were then taken to provide an index for correlation with line elevation and other parameters. The first step in the computation of V_E was the evaluation of v_y, the velocity at a point a distance y above the streambed, using the available velocity data.

The equation generally used for computation of the velocity distribution in turbulent flow is the so-called Prandtl-von Karman universal-velocity-distribution law (Chow, 1959, p. 201),

$$v_y = 2.5V_f \ln \frac{y}{Y_o}, \tag{1}$$

where

v_y = the point velocity at a distance y above the bottom of the stream,

V_f = the friction velocity or shear velocity at the boundary, and

Y_o = a constant related to Z_f and the kinematic viscosity of the fluid.

A less precise, but generally accepted, premise is that the velocity distribution may be approximated by the so-called power-law equation,

$$v_y = ky^m \tag{2}$$

where k and m are numerical constants.

Equation 2 lends itself more easily to manipulation and has been used in the following computations because precise definition of the more sophisticated relation cannot be made under the flow conditions encountered in a channel subject to unsteady flow. Energy and momentum changes under these conditions are of much greater significance than boundary and viscosity factors, and precise definition of V_f and Y_o is impractical. The formula for computing the exponent m is derived below. The symbols listed refer to those used in figure 4.

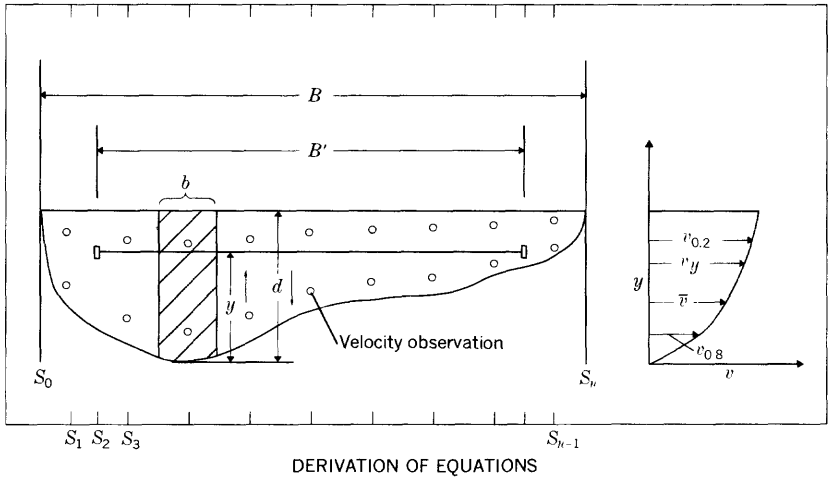

DERIVATION OF EQUATIONS

FIGURE 4.—Typical velocity data. Symbols defined in text.

Assuming that the vertical-velocity distribution follows the power law, then $\bar{v}$, the mean velocity in a given vertical, can be computed as:

$$\bar{v}=\frac{1}{d}\int_0^d v_y dy=\frac{1}{d}\int_0^d ky^m dy$$

$$=\frac{1}{d}\left[\frac{k}{m+1}\,y^{(m+1)}\right]_0^d=\frac{kd^m}{m+1} \tag{3}$$

where

d= the depth of water in the vertical,

$y=0.8d$ for $v_{0.2}$, a velocity observation at 0.2 of the depth below the water surface,

and

$y=0.2d$ for $v_{0.8}$, a velocity observation at 0.8 of the depth below the water surface.

Thus, from equation 2,

$$v_{0.2}=k(0.8d)^m$$

and

$$v_{0.8}=k(0.2d)^m,$$

and

$$\frac{v_{0.8}}{v_{0.2}}=\frac{k(0.2d)^m}{k(0.8d)^m}=0.25^m,$$

or

$$m=\frac{\log\left(\frac{v_{0.8}}{v_{0.2}}\right)}{\log 0.25}. \tag{4}$$

If $\bar{v}$ is assumed equal to the average of $v_{0.2}$ and $v_{0.8}$, a good approximation of v_y can be computed from equations 2 and 3, and the value of m computed from equation 4. This assumption, commonly made in field practice, is not compatible with the use of the power-law velocity distribution, but the error introduced is small. Thus, from equations 2 and 3,

$$\frac{v_y}{\bar{v}}=\frac{ky^m}{\frac{kd^m}{m+1}}=(m+1)\left(\frac{y}{d}\right)^m,$$

or

$$v_y=\bar{v}(m+1)\left(\frac{y}{d}\right)^m \tag{5}$$

An average value ($\overline{m}$) of the exponent m can be computed as follows. For a given subsection

$$(q_{0.2_i})=(v_{0.2})_i a_i,$$

and

$$Q_{0.2}=\sum_{i=1}^{n}[(v_{0.2})_i(a)_i]=\overline{V}_{0.2}A \tag{6}$$

where

a = area associated with the subsection,

A = total area in cross section,

i = subsection number,

$q_{0.2}$ = discharge in subsection computed from $v_{0.2}$, and

$Q_{0.2}$ = total discharge in stream computed on the basis of velocity observations at the 0.2 depth.

Note: $Q_{0.2}$ and $q_{0.2}$ have no physical meaning, but provide a convenient device for computing the weighted mean value of $v_{0.2}$.

The total discharge is normally computed as:

$$Q=\sum_{i=1}^{m}\left[\frac{v_{0.2}+v_{0.8}}{2}\right]_i a_i,$$

which can be manipulated to

$$Q=\left[\frac{\overline{V}_{0.2}+\overline{V}_{0.8}}{2}\right]A \tag{7}$$

where

Q = total discharge in the cross section,

$V_{0.2}$ = weighted average of $v_{0.2}$ in the cross section, and

$V_{0.8}$ = weighted average of $v_{0.8}$ in the cross section.

From equations 6 and 7,

$$\frac{Q}{Q_{0.2}}=\frac{\overline{V}_{0.2}+\overline{V}_{0.8}}{2\overline{V}_{0.2}},$$

and

$$\overline{V}_{0.8}=2\overline{V}_{0.2}\left(\frac{Q}{Q_{0.2}}\right)-\overline{V}_{0.2},$$

and

$$\frac{\overline{V}_{0.8}}{\overline{V}_{0.2}}=2\left(\frac{Q}{Q_{0.2}}\right)-1 \tag{8}$$

Substituting in equation 4,

$$\overline{m}=\frac{\log\frac{\overline{V}_{0.8}}{\overline{V}_{0.2}}}{\log 0.25}=\frac{\log\left[2\left(\frac{Q}{Q_{0.2}}\right)-1\right]}{-0.60206} \tag{9}$$

Computation of average line velocities (V_E) was based on the assumption that derived point velocities (v_y) were applicable over the distance b of each related subsection.

$$V_E=\frac{v_{y_1}b_1+v_{y_2}b_2+\ldots v_{y_n}b_n}{b_1+b_2+\ldots b_n}=\frac{\sum_{i=1}^{n}[(v_y)_i b_i]}{B} \tag{10}$$

where

V_E=average velocity along a line at an elevation E in the cross section,

b=subsection width,

B=total width,

and

$$(v_y)_i=\bar{v}_i\left[(\bar{m}+1)\left(\frac{y_i}{d_i}\right)^{\bar{m}}\right] \tag{11}$$

where

y=selected line elevation minus subsection bottom elevation,

d=subsection depth,

and, from current-meter data at subsection,

$$\bar{v}=\frac{v_{0.2}+v_{0.8}}{2}.$$

CORRELATION BETWEEN AVERAGE LINE VELOCITY AND MEAN VELOCITY IN CROSS SECTION

Underwater components of an AVM must be located in deep water, and in most channels this will require that they be at some distance from either bank. In consequence, the line velocity (V_E) across the entire stream cannot be measured. However, because the undefined shallow end sections carry only a small part of the total flow, a valid index of flow conditions can be obtained by determining V_E over the deep central part of the channel.

For the present analysis the end points of the acoustic path were assumed to be located at S_2 and S_{n-2}, shown in figure 4. Computations of V_E were based on an evaluation of the exponent $\bar{m}$ from computations of $Q_{0.2}$ and Q in the net section of width B'. The end product of the analysis is expressed in the ratio (C) of the mean velocity in the total cross section to the computed line velocity along the assumed acoustic path.

$$C=\frac{\overline{V}}{V_E} \tag{12}$$

where

$V=Q/A$ for total cross section, and

V_E=line velocity over width B'.

This ratio is comparable to the coefficient required to convert line velocities, such as those that will be obtained from an AVM, into equivalent mean velocities in the cross section. The differences are that these computations are based entirely on current-meter measurement data and relate to a cross section normal to the streamlines of flow rather than to one placed diagonally across the channel.

Values of C (eq 12) were computed for various path elevations on an hourly basis using the discharge measurements discussed previously. Consistency of the computed values was good, except during the short periods near slack water when the flow regime is unstable. Duration of such slow, unstable flow is relatively short, as can be seen by reference to figure 3. Discharge may change from an ebbflow of 75,000 cfs to a floodflow of equal magnitude in less than 1 hour, and discharges during these transition periods probably can be computed more accurately by interpolation between the periods when the flow streamlines are stable than by any other technique. It was concluded, therefore, that definition of C during transition periods was of no value, and results for periods when mean velocities were less than 0.6 fps (feet per second) were accordingly excluded from the analysis.

The overall means and standard deviations of the C values were computed for each path elevation. Results are tabulated in table 1 and plotted in figures 5 and 6. Figure 5 shows that C increases with depth, as would be expected, and reaches unity at an elevation of about 19 feet below the assumed datum. Of more interest is the variation of the standard deviation of C shown in figure 6. A high standard deviation results from paths selected near the top or the bottom, whereas the least deviation results when the path is about 17 feet below the assumed datum. At an elevation of 17.4 feet below the assumed datum, $\overline{C}$ was 0.993 and the standard deviation of C was 0.026. That elevation was, therefore, considered optimum for measuring line velocity, and velocity computations for that elevation were

TABLE 1.—*Average values and standard deviation of* C

Path elevation below assumed datum (ft)	Number of computed values	Average C	Standard deviation of C
2. 35	26	0. 939	0. 112
6. 35	26	. 950	. 091
11. 35	26	. 968	. 059
15. 4	108	. 984	. 030
16. 4	69	. 989	. 026
17. 4	108	. 993	. 026
19. 4	108	1. 003	. 033
21. 4	65	1. 019	. 061

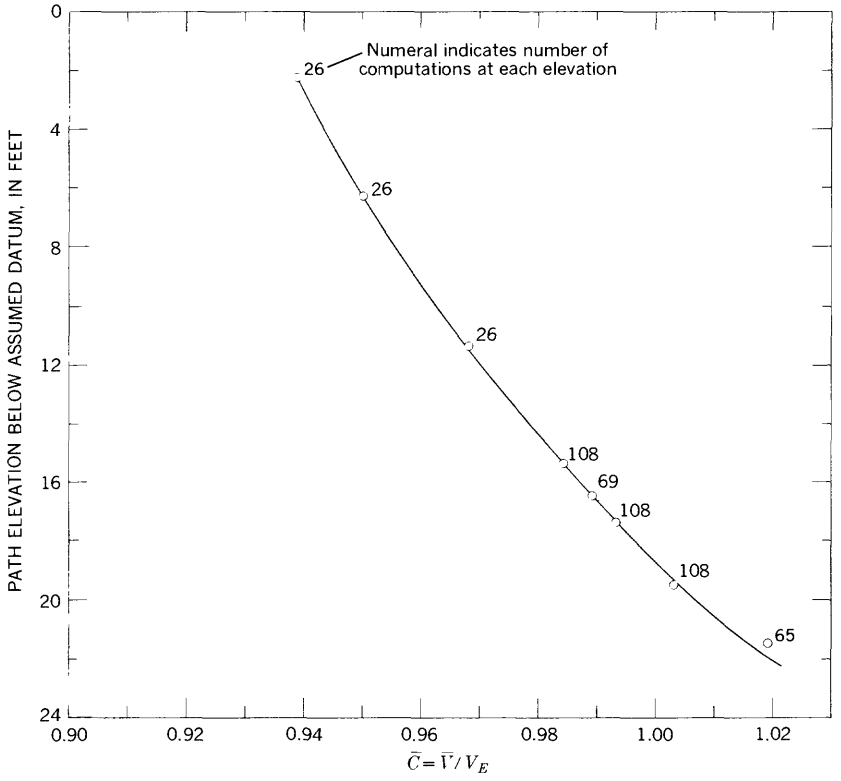

FIGURE 5.—Relation between $\bar{C}$ and path elevation.

used in the subsequent study of the stability of the relation between line velocity and mean velocity in the cross section.

Departures of the individual C values at the 17.4-foot elevation below the assumed datum were checked for randomness by applying the statistical test of runs (Dixon and Massey, 1957). With 108 items there were 38 runs, indicating that the variations about the mean did not occur randomly in time. In consequence, analysis was directed toward determining parameters which might explain this nonrandom scatter. Variation of C with the following parameters was investigated: Gage height, mean velocity, rate of change of gage height, rate of change of velocity, salinity variations, and phase of tidal cycle. A consistent relation was found between C and velocity variations within each phase of the tidal cycle. No other correlations could be established.

The tide cycle was divided into four phases—increasing ebb, decreasing ebb, increasing flood, and decreasing flood—and arithmetic mean C values were computed from data, grouped according to velocity, within each of these phases. Table 2 summarizes these

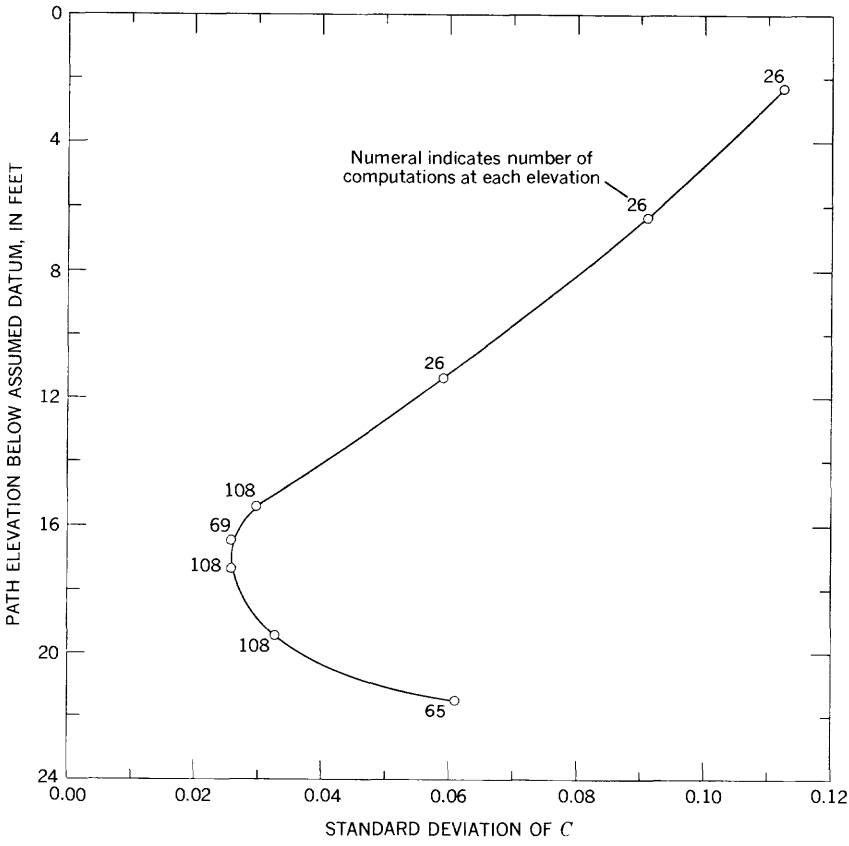

FIGURE 6.—Relation between standard deviation of C and path elevation.

TABLE 2.—*Variation of* C *with tidal phase*

Velocity range (fps)	Increasing ebb			Decreasing ebb			Increasing flood			Decreasing flood		
	$\overline{V}$ (fps)	$\overline{C}$	s	$\overline{V}$ (fps)	$\overline{C}$	s	$\overline{V}$ (fps)	$\overline{C}$	s	$\overline{V}$ (fps)	$\overline{C}$	s
<1.00	0.90	0.961	(1)	0.84	1.03	0.031	0.87	1.005	0.030			
1.00–1.40	1.16	.957	0.035				1.21	1.006	(1)	1.11	0.983	(1)
1.41–1.80	1.52	.965	(1)	1.41	1.040	(1)	1.75	.982	(1)	1.58	.997	0.022
1.81–2.20	1.96	.981	.011	2.02	1.019	.017	2.09	.970	(1)	2.08	.991	.020
2.21–2.60	2.44	.978	.014	2.46	1.019	.018	2.43	.985	.011	2.43	.992	.009
>2.60	2.75	.985	.009	2.76	.990	.014	2.92	.982	.007	2.84	.982	.009

[1] Only one or two values used to obtain $\overline{C}$.

computations. Figure 7 is a plot of the data, using an abscissa which runs from 0 to 3 fps for increasing ebb, from 3 to 0 fps for decreasing ebb, from 0 to −3 fps for increasing flood, and from −3 to 0 fps for decreasing flood. Use of this abscissa poses a problem when maximum

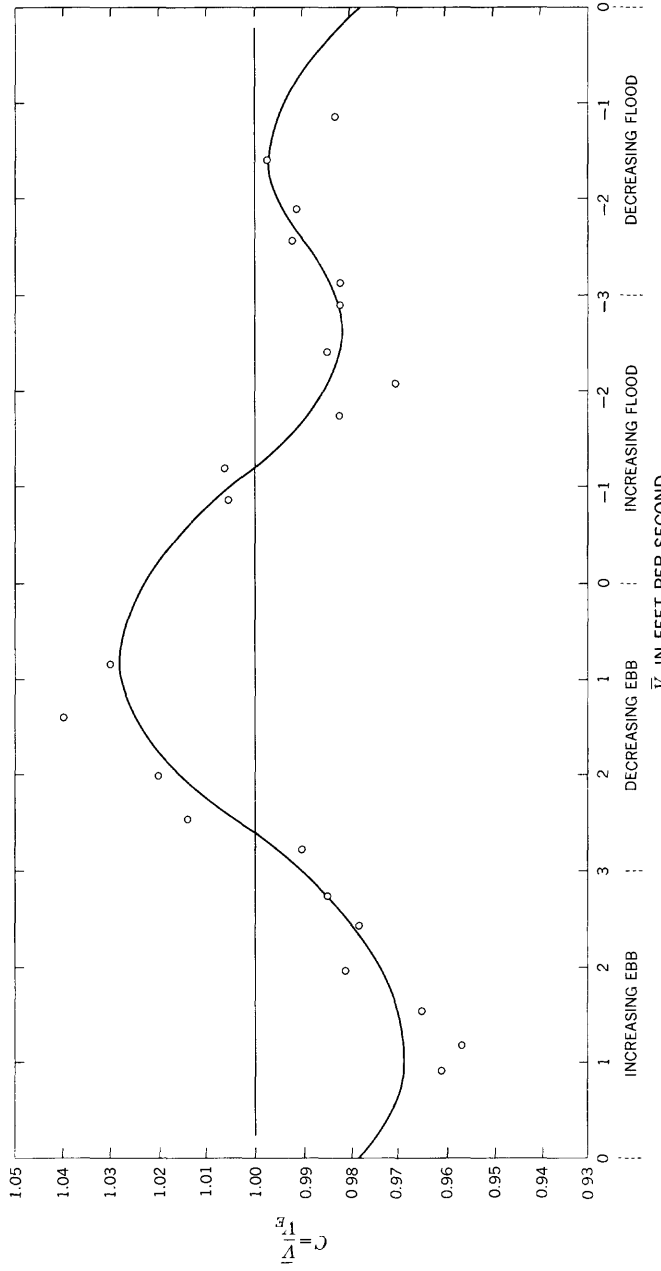

FIGURE 7.—Relation between C and velocity and tide phase.

velocities within a cycle are appreciably greater than 3 fps, but this deficiency could be rectified by substituting an abscissa in terms of the ratio of instantaneous recorded velocity to the maximum observed within a cycle. Such a refinement was not considered necessary for this analysis, but it could be applied for computer computations.

Discharges occurring during periods of the tidal cycle when velocities are high contribute the major part of the water flowing during each ebb and flood cycle, and, in consequence, the C values applied during the high-velocity periods are of more importance than those used during periods of low velocity. The use of an average C value, weighted relative to velocity, therefore seems a logical alternative to the use of a flat average or of a relation such as that shown in figure 7.

Average values of C weighted relative to velocity by the formula

$$\bar{C}=\frac{\Sigma C\overline{V}}{\Sigma V}$$

were computed for the total cycle, for overall ebb and flood periods, and for each of the four tidal phases. Table 3 summarizes these computations.

TABLE 3.—*Weighted average* C *values*

Period	$\bar{C}$	Standard deviation of C
Total cycle	0.990	0.015
Ebb cycle	.993	.028
Flood cycle	.988	.022
Increasing ebb cycle	.975	.018
Decreasing ebb cycle	1.010	.023
Increasing flood cycle	.988	.045
Decreasing flood cycle	.988	.018

Computations of C values and of the relation between C and tidal phase shown in figure 7 were based upon data for the period September 12–16, 1954. To provide some insight into the relative merit of alternative computation methods, hourly computations of flow were made by applying coefficients from figure 7 and those summarized in table 3 to line velocities computed from current-meter data for the subsequent period, September 20–24, 1954.

Mathematical relations are as follows:

$$Q_M=\sum_{i=1}^{n}\left[\left(\frac{v_{0.2}+v_{0.8}}{2}\right)_i a_i\right],$$

from current-meter measurements

$$Qc=C\overline{V}_E A$$

where

Q_M = measured discharge,

Qc = discharge computed on basis of line velocity,

C = ratio of mean velocity in the cross section to a mean line velocity as defined by one of four methods listed in table 4,

i = subsection number,

V_E = average line velocity computed from current-meter data using equations 10 and 11, and

A = total area of cross section.

The four sets of computed discharge figures are given in table 4. Discharges shown are averages for the 111-hour period beginning 0700 September 20 and ending 2200 September 24, 1954. As no attempt was made to determine whether these end points represent times of equal storage volume in the upstream delta channels, the computed freshwater outflow is not necessarily a representative figure. However, it does have significance in relation to possible accuracy of flow computations based upon the techniques under study.

Figures in table 4 suggest that accurate determinations of ebb or flood flows in this tidal channel may be made on the basis of an observed line velocity and that meaningful computations of net outflow might also be made. However, no real evidence is presented as to which computation method (1, 2, 3, or 4) should be used. The apparent superiority of method 3, which employs two values of C, 0.993 for

TABLE 4.—*Comparison of measured and computed flows for period 0700 September 20 to 2200 September 24, 1954*

Method	Ebbflow		Floodflow		Outflow	
	Cubic feet per second	Percent difference from measured flow	Cubic feet per second	Percent difference from measured flow	Cubic feet per second	Percent difference from measured flow
Measured Q	112, 800	----	108, 500	----	4, 300	----
Computed Q by method 1[1]	113, 100	+0. 3	108, 000	−0. 5	5, 100	+19
Computed Q by method 2[2]	111, 400	−1. 2	108, 200	−. 3	3, 200	−26
Computed Q by method 3[3]	111, 100	−. 8	107, 400	−1. 0	4, 500	+5
Computed Q by method 4[4]	113, 100	+. 4	107, 400	−1. 0	5, 700	+33

[1] Method 1, C based on tide cycle phase and velocity from figure 7.
[2] Method 2, C=0.990 for total tidal cycle.
[3] Method 3, C=0.993 for ebb cycle, 0.988 for flood cycle.
[4] Method 4, C=0.988 for flood cycle, 0.975 for increasing ebb cycle, and 1.010 for decreasing ebb.

ebbflows and 0.988 for floodflows, is probably fortuitous. Method 1, using a C value related to velocity and tidal phase, is a logical treatment of the variables in the problem, and this type of procedure probably holds the greatest promise. Standard deviation of departures of C values from the curve in figure 7 is 0.026.

ACOUSTIC-VELOCITY-METER CHARACTERISTICS

BASIC THEORY

Several AVM systems have been developed using minor variations of the same basic theory. The technique of measuring the velocity of the water by determining the traveltimes of sound pulses moving in both directions along a diagonal path between transducers (sound generators and receivers) near each bank is common. The water velocity indicated by the instrument is the average velocity component parallel to the acoustic path, the line between the two transducers.

Derivation of basic equations for the AVM system developed by the U.S. Geological Survey, in cooperation with the U.S. Army Corps of Engineers and the California Department of Water Resources, can be made as follows: For the geometry and flow direction shown in figure 8,

$$T_{AB}=\frac{B}{c-V_E}, \text{ or } c-V_E=\frac{B}{T_{AB}}, \tag{13}$$

$$T_{BA}=\frac{B}{c+V_E}, \text{ or } c+V_E=\frac{B}{T_{BA}}. \tag{14}$$

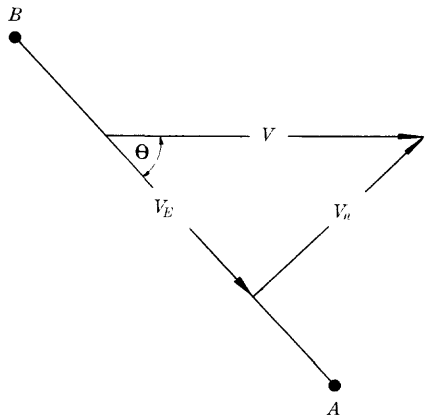

FIGURE 8.—Acoustic-velocity-meter principles.

Combining equations 13 and 14,

$$V_E=\frac{B}{2}\left[\frac{1}{T_{BA}}-\frac{1}{T_{AB}}\right], \tag{15}$$

and

$$c=\frac{B}{2}\left[\frac{1}{T_{BA}}+\frac{1}{T_{AB}}\right] \tag{16}$$

where

V_E=average water velocity along the acoustic path on the horizontal line from A to B,
T_{BA}=traveltime of an acoustic signal from B to A,
T_{AB}=traveltime of an acoustic signal from A to B,
c=propagation rate of sound in still water, and
B=length of acoustic path.

Computation of discharge in a large channel, such as that at the Chipps Island site, can best be done by use of A_p, the cross-sectional area parallel to the acoustic path. To satisfy the basic equation $Q=A\overline{V}$, the velocity component normal to this cross section (V_n) must be used. From the geometry shown in figure 8

$$V_n=V_E \tan \theta \tag{17}$$

where θ is the angle of departure between the streamlines of flow and the acoustic path. This index velocity, V_n, must also be corrected by the coefficient C, discussed earlier, to equate it to the mean velocity in the cross section. The equation applicable to discharge computations is, thus,

$$Q=A_pCV_n, \tag{18}$$

which, by substituting from equations 15 and 17, becomes

$$Q=\frac{A_pC\tan\theta B}{2}\left[\frac{1}{T_{BA}}-\frac{1}{T_{AB}}\right]. \tag{19}$$

The accuracy of flow computations is thus dependent upon the precision with which the factors A_p, C, θ, B, T_{BA}, and T_{AB} can be defined.

EFFECT OF VARIATION IN STREAMLINE ORIENTATION

Flow conditions in the Chipps Island channel are affected by the slight curvature of the reach and by the configuration of the bays that lie at either end. Floodflows enter the west end of the channel from the broad expanse of Suisun and Honker Bays; ebbflows enter on the east from the narrow upper part of Suisun Bay at the confluence of the Sacramento and San Joaquin Rivers. There is a curvature of about 10° in the 2½ mile channel.

To define the flow pattern in this channel, an investigation was made during ebb and floodflows on February 11, 1965. Drogues were placed in the channel just prior to the peak of each tide phase, and aerial photographs were taken at 5- to 10-minute intervals from an altitude of 4,800 feet. Drift of the drogues with the current was traced through these sequent exposures, and the streamline patterns shown in figure 9 were defined. Drogues employed were 2-foot-square styrofoam floats supporting a 10-quart bucket placed 15–20 feet below the water surface.

The average bearing of streamlines for flow during the ebbtide differs by 5°30′ from that during the floodtide. The indicated difference may have been due in part to wind during the test period; there was a moderate wind from the north during both observation periods which undoubtedly caused the drogues to drift toward the south shore. Therefore, actual differences are probably less than the 5° recorded, but significant variations in streamline bearing must be expected between ebbflow and floodflow periods. This difference in streamline orientation will have little significance if the pattern during successive tidal cycles is repetitive. If so, changes that occur between ebb and flood periods will be defined during the current-meter measurement program required for calibration. However, if there are random, undetected variations in flow pattern after the calibration period such as might be caused by wind or changes in the proportions of flow contributed by the Sacramento and San Joaquin Rivers, then the value of θ will be uncertain, and the accuracy of flow computations will be affected.

An evaluation of the magnitude of errors resulting from undefined changes in θ can be made by application of equation 19. Referring to figure 10, assume that θ is the angle of departure defined during calibration, but the actual angle of departure, resulting from high winds, is $\theta + \phi$. The computed discharge (Q) from equation 19 is

$$Q=\frac{A_v C \tan \theta B}{2}\left[\frac{1}{T_{BA}}-\frac{1}{T_{AB}}\right]. \tag{19}$$

The actual discharge (Q') should be

$$Q'=\frac{A_v C \tan (\theta+\phi) B}{2}\left[\frac{1}{T_{BA}}-\frac{1}{T_{AB}}\right]. \tag{20}$$

The ratio between Q and Q' from equations 19 and 20 is

$$\frac{Q}{Q'}=\left[\frac{\tan \theta}{\tan (\theta+\phi)}\right]. \tag{21}$$

A numerical evaluation of equation 21 for various angles of θ and ϕ is given in table 5. This table indicates that computed discharges will be too small when the assumed angle of departure (θ) is less than the actual angle ($\theta+\phi$), and that, conversely, the computed discharge will be too large when the assumed angle of departure is greater than that which actually occurs. If ϕ is constant for flows in both directions, errors will be of the same sign, and the effect on the computed net outflow will be of the same percentage. However, if ϕ varies between ebb and flood flows, which is to be expected in this channel, errors will not be equal, and the error introduced into the computed net outflow will be very large.

The preceding discussion has referred to an acoustic-velocity-metering system employing a single acoustic path. However, if a system using two paths, as illustrated in figure 11, is used, errors due to variation of ϕ will tend to cancel providing $\phi_{AB} \cong \phi_{AC}$. Errors will be positive for one path and negative for the other.

If the orientation of the two paths is such that $\theta_{AB}=\theta_{AC}$, and streamlines do not change between the two paths, the overall effects of variations in ϕ will be as listed in table 6. Discharges computed as an average of the indicated flows for the two paths will be consistently larger than the true discharge whenever the actual angle of departure ($\theta+\phi$) differs from the assumed angle of departure (θ), but the errors will be small and nonadditive for ebbtide and floodtide phases. However, if there is a significant curvature in the streamlines, then ϕ_{AB} may not equal ϕ_{AC}, and fairly large errors may result, as shown in table 7. Ideally, the average angles of departure should be the same for both paths, and variations from this assumed orientation should balance during each tidal phase.

TABLE 5.—*Variation of ratio* Q/Q′ *with* ϕ *for single path system*

θ	ϕ									
	+5°	+4°	+3°	+2°	+1°	−1°	−2°	−3°	−4°	−5°
30°	0.825	0.856	0.889	0.924	0.961	1.042	1.086	1.133	1.184	1.238
40°	.839	.869	.900	.932	.965	1.036	1.074	1.114	1.155	1.198
45°	.839	.869	.900	.932	.966	1.036	1.072	1.111	1.150	1.192

TABLE 6.—*Variation of ratio* Q/Q′ *with* ϕ *for two-path system where* $\theta_{AB}=\theta_{AC}$

θ	ϕ									
	+5°	+4°	+3°	+2°	+1°	−1°	−2°	−3°	−4°	−5°
30°	1.032	1.020	1.011	1.004	1.002	1.002	1.004	1.011	1.020	1.032
40°	1.018	1.012	1.007	1.003	1.001	1.001	1.003	1.007	1.012	1.018
45°	1.015	1.010	1.005	1.002	1.001	1.001	1.002	1.005	1.010	1.015

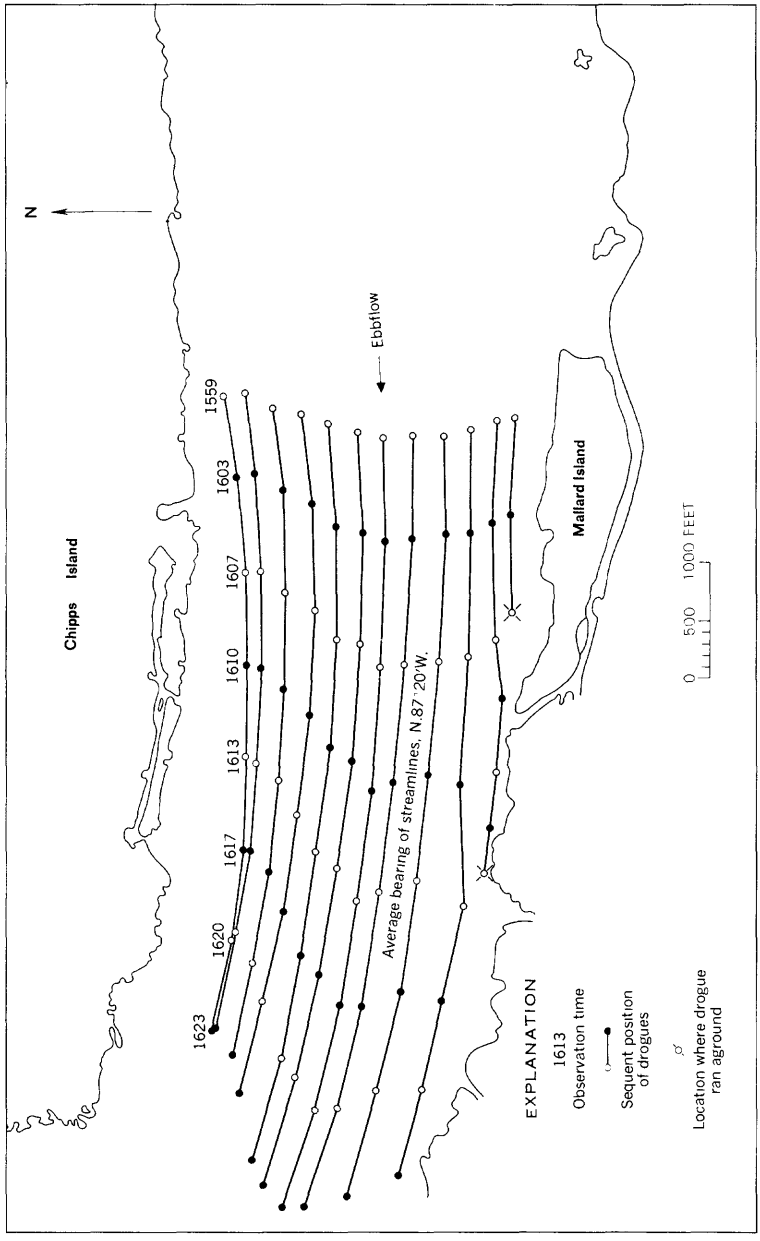
N
Chipps Island
Ebbflow
1559
1603
1607
1610
1613
1617
1620
1623
Average bearing of streamlines, N.87°20'W.
Mallard Island
0 500 1000 FEET
EXPLANATION
1613
Observation time
Sequent position of drogues
Location where drogue ran aground

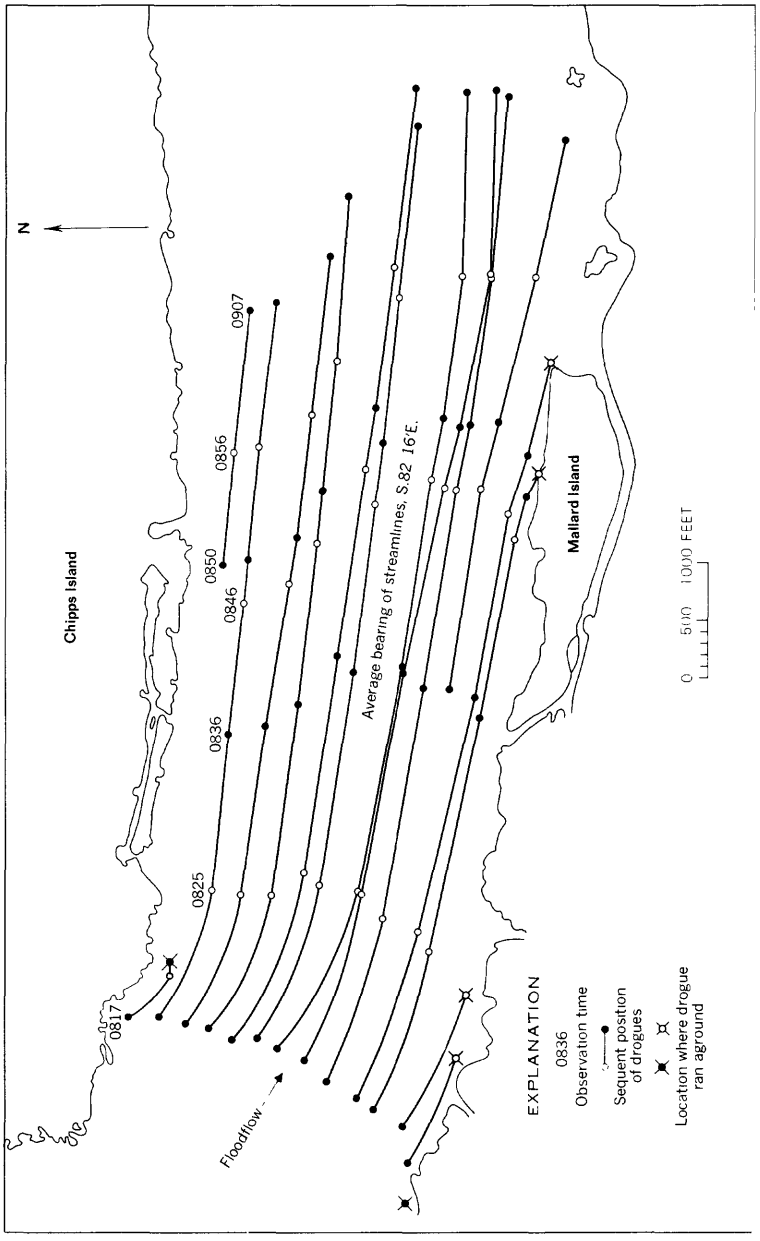

FIGURE 9.—Streamlines in Chipps Island channel during period of ebbflow (upper map) and floodflow (lower map), February 11, 1965.

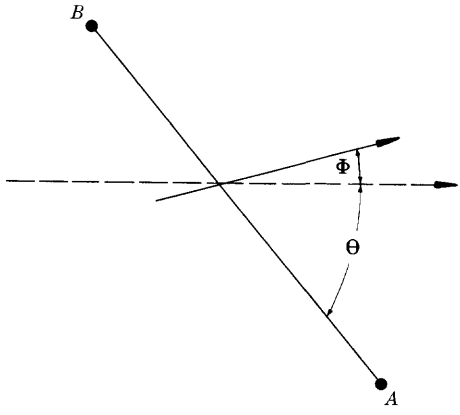

FIGURE 10.—Errors in θ.

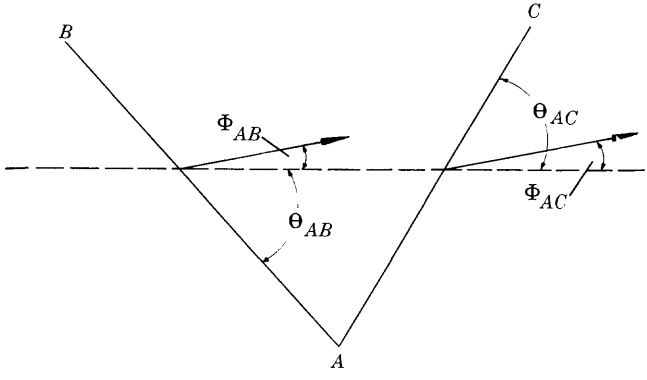

FIGURE 11.—Acoustic-velocity-meter system using two paths.

TABLE 7.—*Variation of ratio Q/Q' for two-path system when* $\theta=45°$ *and* $\phi_{AB} \neq \phi_{AC}$

ϕ_{AB}	ϕ_{AC}					
	0°	1°	2°	3°	4°	5°
0°	1. 000	1. 018	1. 036	1. 055	1. 075	1. 096
1°	. 983	1. 001	1. 019	1. 038	1. 058	1. 079
2°	. 966	. 984	1. 002	1. 022	1. 041	1. 062
3°	. 950	. 968	. 986	1. 005	1. 025	1. 046
4°	. 935	. 952	. 971	. 990	1. 010	1. 031
5°	. 920	. 937	. 956	. 975	. 995	1. 015

EFFECT OF ERRORS IN TIMING

Accuracy of discharge computations must be related also to the precision with which the traveltimes of the acoustic signal (T_{AB} and T_{BA} in eq 19) can be measured. Factors involved here relate directly to the characteristics of the various components of the system.

The basic timing unit, a crystal-controlled oscillator, has an accuracy of one part in 10^7 parts. However, the interrelation of characteristics of the sound transducers, hydrophones, amplifiers, and the trigger circuitry in the time-interval counter make it impossible to achieve an overall accuracy of the same precision.

The net effect of the system characteristics is that the recorded traveltimes are consistently greater than the actual traveltimes by a small increment, ΔT. Thus, $T_{AB}=T'_{AB}-\Delta T_A$ and $T_{BA}=T'_{BA}-\Delta T_B$, where T'_{AB} and T'_{BA} are the recorded times. If the increments ΔT_A and ΔT_B are the same, then no significant error is introduced into computation of V_E. This is so because V_E is computed from the difference in the reciprocals of the indicated times of travel, and ΔT is small relative to T'_{AB} or T'_{BA}. However, if signal strength in either direction varies, due to changes in the performance of system components or to changes in water quality, then ΔT_A may be different from ΔT_B, and an error, biased as to flow direction, will result.

Experience with the AVM on the Delta-Mendota Canal near Tracy, Calif., has indicated that the difference between ΔT_A and ΔT_B can be as great as 10 μsec (microseconds). The best performance, covering the period March 4–30, 1965, yielded an average value of $\Delta T_A-\Delta T_B$ equal to -0.7 μsec with a standard deviation of 3.0 μsec. These computations were based on comparison of line velocities defined by current-meter measurements with line velocities conputed from the AVM output data. It should be noted that for the system at Tracy the standard deviation of 3.0 μsec. converted into an equivalent velocity range represents a ± 3.0 percent velocity variation.

The AVM system at Tracy has a path length of 600 feet, and, consequently, there is some hazard in extrapolating results from this site to a system at Chipps Island, where path lengths would be about 4,000 feet. However, if performance equal to that experienced at Tracy can be achieved, then time differentials ($\Delta T_A-\Delta T_B$) of about 5–10 μsec can be expected. A 10 μsec differential will cause an error of about 1 percent over a path length of 4,000 feet—an error which seems very small for total flow computation. However, this error would result in much larger errors in the computed net outflow, because the error would be positive for flow in one direction and negative for flow in the reverse direction.

EFFECT OF VARIATIONS IN SALINITY AND TEMPERATURE

Derivation of equation 15 was made on the assumption that c, the propagation rate of sound in still water, was constant throughout the cross section. This assumption requires that the temperature and salinity of the water be uniform along the acoustic path at any given time. If there is a significant gradient in temperature or salinity, velocities indicated by an AVM may be in error.

Evaluation of the effect of nonhomogeneity in water temperature and salinity can be made by manipulation of equations 13, 14, and 16, and a detailed study of the significance of this factor was made using temperature and salinity data included in the measurement report of the Water Project Authority of the State of California (1955). That study, details of which are not included here, indicated that there was no significant variation of temperature in the cross section and that lateral variations of salinity concentration of as much as 1,500 mg/l (milligrams per liter), the largest recorded in the channel, would have no significant effect on the computed results. Therefore, errors from those sources can be ignored in overall accuracy evaluation.

EFFECT OF VARIATION IN SUSPENDED-SEDIMENT CONCENTRATION

The attenuation of an ultrasonic wave passing through a fluid is greater when suspended particles are present than when they are absent. The amount of attenuation is a function of particle size, density, and concentration, fluid viscosity and density, the frequency of the acoustic signal, and the length of the sound path.

Equations given by Flammer (1962) for evaluation of energy loss are:

$$E=E_0 10^{-0.1\alpha x} \tag{22}$$

where

E=sound energy flux at a given point, if sediment is suspended in the transmitting fluid;

E_o=sound-energy flux at the same point, if no sediment were present;

α=attenuation coefficient that is due to sediment alone, measured in decibels per inch; and

x=distance from the point of measurement to the sound source.

The attenuation coefficient α can be evaluated as

$$\alpha=C\left[\frac{K(\gamma-1)^2 S}{S^2+(\gamma+\tau)^2}+\frac{K^4 r^3}{6}\right]\frac{22.05}{2} \tag{23}$$

where

C=concentration (1,000 mg/l=0.001),

$K=2\pi/\lambda$,

$\gamma=\rho_1/\rho_2$,

$S=[9/(4\beta r)]\ [1+1/(\beta r)]$,

$\tau=\frac{1}{2}+9/(4\beta r)$, and

r=particle radius, in centimeters,

in which

λ=wave length of sound in water, in centimeters;

ρ_1 and ρ_2=densities of particle and fluid, respectively;

$\beta=[\omega/2v]^{1/2}$;

$\omega=2\pi f$;

v=kinematic viscosity of water, in stokes; and

f=frequency of sound wave.

The notations above are after Flammer (1962) and apply only to this section of the report; to avoid confusion, they are not included in the list of symbols for the present report.

Data on concentration and size distribution of suspended sediment in the Chipps Island channel have not been obtained, but reasonable estimates of the probable range can be made on the basis of records at inflow stations. Velocities in the delta channels are not high enough to keep coarse materials in suspension, so it is safe to assume that the bulk of suspended material reaching Chipps Island is composed of fine silt and clay in the size range of less than 0.008 mm (millimeter). At the inflow station on the Sacramento River at Sacramento, about two-thirds of the suspended material is in this size range; most of this material is carried through the delta and deposited in San Francisco Bay. The mean daily concentration range in the Sacramento River at Sacramento during the 1964 water year was from 22 mg/l to 494 mg/l, but on only 22 days during the year was it greater than 100 mg/l. Therefore, concentrations in the Chipps Island channel will probably seldom exceed 100 mg/l and will generally be less than 50 mg/l. Size of material will almost always be less than 0.008 mm and will more likely be about 0.004 mm.

Evaluation of equations 22 and 23 for sediment loads in this probable concentration and size range is shown in figure 12. Figure 12*A* illustrates the general problem and shows the reduction in signal strength resulting from sediment loads ranging from 50 mg/l to 400 mg/l over acoustic paths as long as 4,000 feet. Figure 12*B* shows the signal loss for a given concentration and path length, as affected by particle size, and relates signal loss, for a path length of 4,000 feet, to sediment size when the sediment concentration is held constant at 100 mg/l. Figure 12*C* relates signal loss, for a path length of 4,000 feet, to sediment concentration when the sediment size is held constant at 0.004 mm. Figure 12*C* is of particular significance; it indicates that for the probable range in suspended-sediment loads in the Chipps Island channel (20–100 mg/l), signal strength will vary from 90 to 56 percent of the levels possible in clear water. One of the requirements of an AVM designed for use at this site would be that no calibration changes should result from signal strength variations of this magnitude. This is considered possible, but it is not true of the USGS (U.S. Geological Survey) system.

FIELD TESTS OF U.S. GEOLOGICAL SURVEY ACOUSTIC VELOCITY METER

CHIPPS ISLAND CHANNEL

Investigations at the AVM test site on the Delta-Mendota Canal near Tracy, Calif., showed that acoustic signals of the character used in the USGS system can be transmitted as far as 2,000 feet. Similar tests made at the Snake River near Clarkston, Wash., site extended the possible transmission range to 6,800 feet. Another test program at the Tracy, Calif., site showed significant attenuation of signal strength when the sound path was placed near the water surface or the bottom of the channel.

The quality of signal transmission that can be achieved in the Chipps Island channel, as affected by distance and elevation of path in the particular cross section, is a significant factor in evaluation of the system capability. A field program was accordingly initiated to determine the quality of signal transmission along the paths that might be employed for a fixed installation. Effects of variation in signal strength with changes in path elevation were investigated as well as variations which might occur from changes in the flow regime. The tests were made during the period January 27–February 2, 1966.

Equipment used for this test program included a transducer unit and its power supply, an oscilloscope for monitoring the outgoing signal, and a portable powerplant mounted on the 30- by 50-foot barge shown in figure 13. Receiving hydrophones, associated ampli-

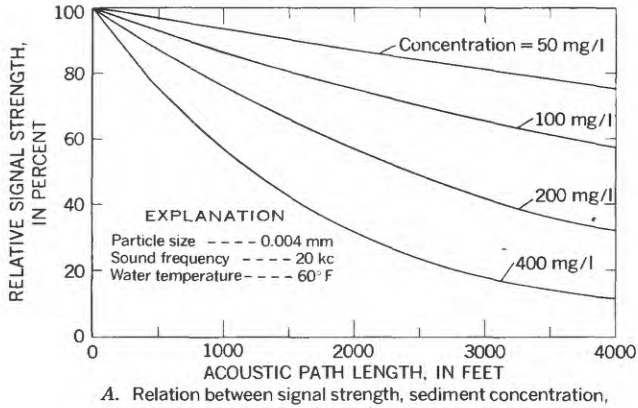

A. Relation between signal strength, sediment concentration, and path length

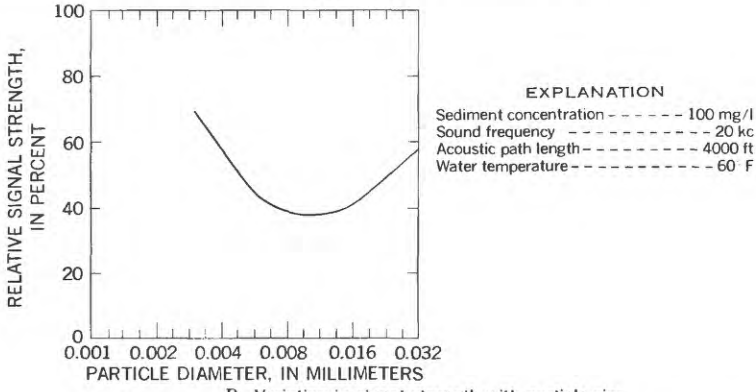

B. Variation in signal strength with particle size

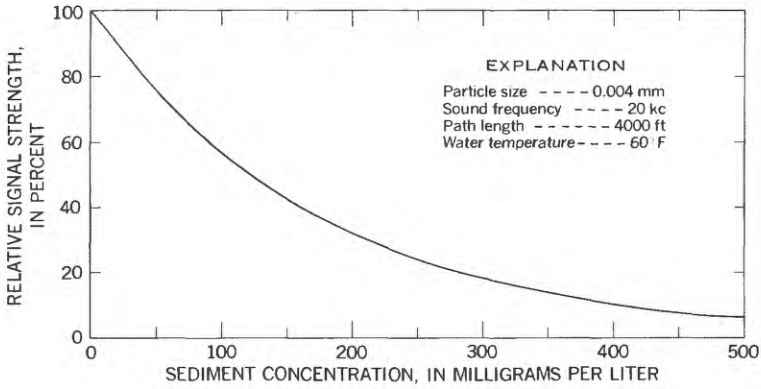

C. Relation between signal strength and sediment concentration

FIGURE 12.—Interrelation between signal strength, sediment concentration, particle size, and acoustic-path length.

FIGURE 13.—Barge and portable laboratory used for field tests.

fiers, a second oscilloscope, and a portable powerplant were mounted on a 21-foot cabin cruiser.

The barge, designed originally as a drilling platform, was equipped with four anchors and winches which permitted accurate positioning and orientation of the unit. An 8- by 8-inch-wide flange section, 40 feet long, was lowered through a 30-inch-diameter well in the center of the barge and secured in position to serve as a vertical track on which the transducer was mounted. A small winch was used to position the transducer at any desired depth to as much as 25 feet below the water surface.

Referring to figure 14, the barge was anchored initially at point *A* and oriented normal to the path *A–C*. The boat was anchored at position *C*. The length of this acoustic path was about 3,700 feet. A series of signal transmission tests was made with the transducer and receiving hydrophones positioned at increasing depths below the water surface. A record of stage was kept so that the elevations of the test paths could be determined. Figure 15 shows the approximate cross sections along paths *A–C* and *B–A′* and the elevations of the acoustic paths employed. Typical received signals are shown in oscilloscope recordings in figure 16. Oscilloscope recordings of at least four signal transmissions were made at each depth, and signal strength, measured as the total voltage swing from minus to plus of the initially recorded pulse, was determined.

Figure 17 shows the variation in signal strength, expressed in percentage of the maximum recorded, plotted against the depth of the acoustic path. Data from tests made along path *B–A′*, discussed

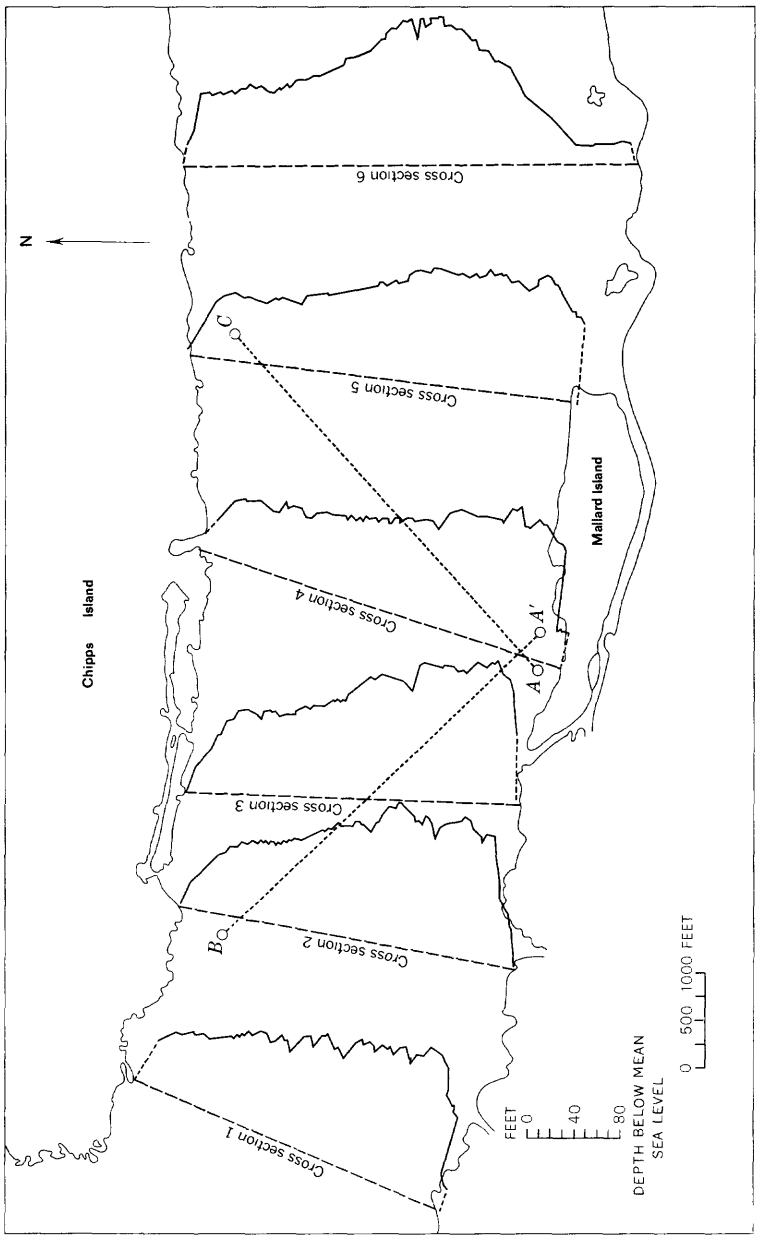

FIGURE 14.—Hydrographic detail at Chipps Island channel.

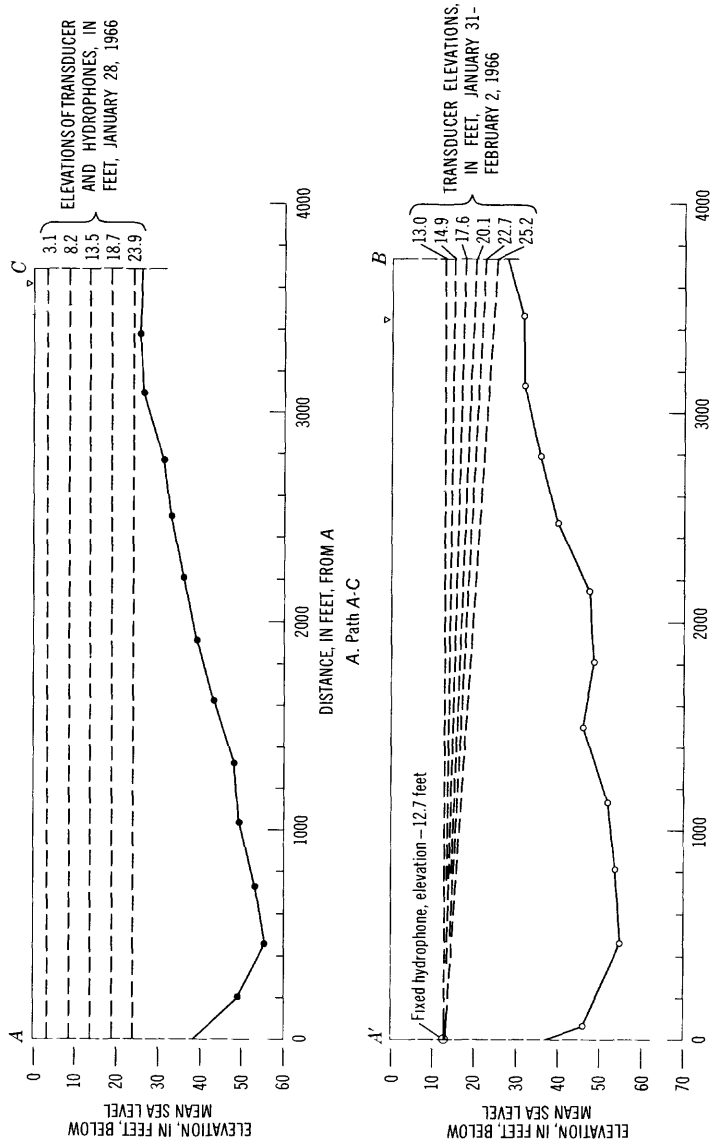

FIGURE 15.—Approximate cross sections along acoustic paths.

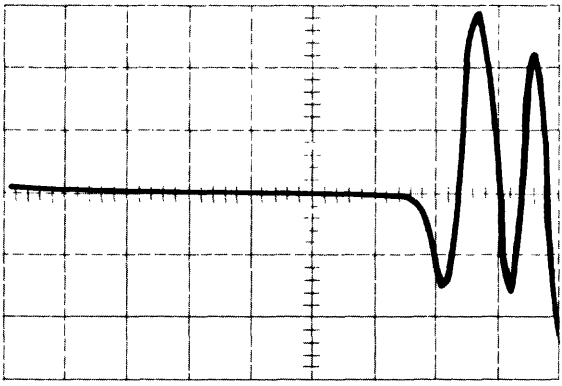

Path *A-C*
Depth 5 feet
Sweep rate 50 μ sec/cm
Vertical scale 1 v/cm

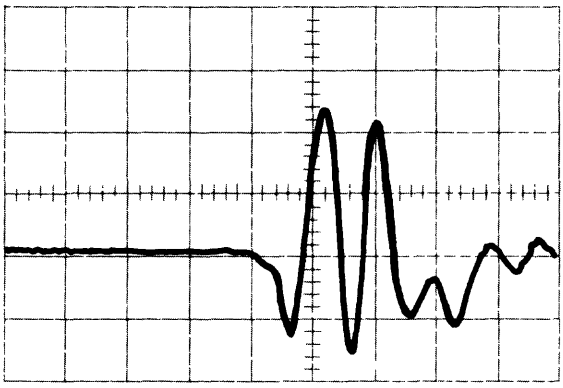

Path *A-C*
Depth 15 feet
Sweep rate 50 μ sec/cm
Vertical scale 2 v/cm

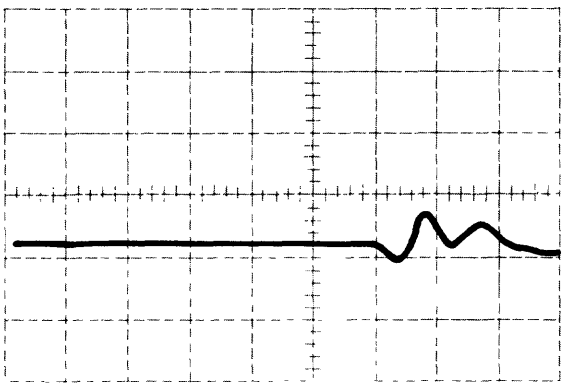

Path *A-C*
Depth 25 feet
Sweep rate 50 μ sec/cm
Vertical scale 2 v/cm

FIGURE 16.—Oscilloscope recordings of typical received signals.

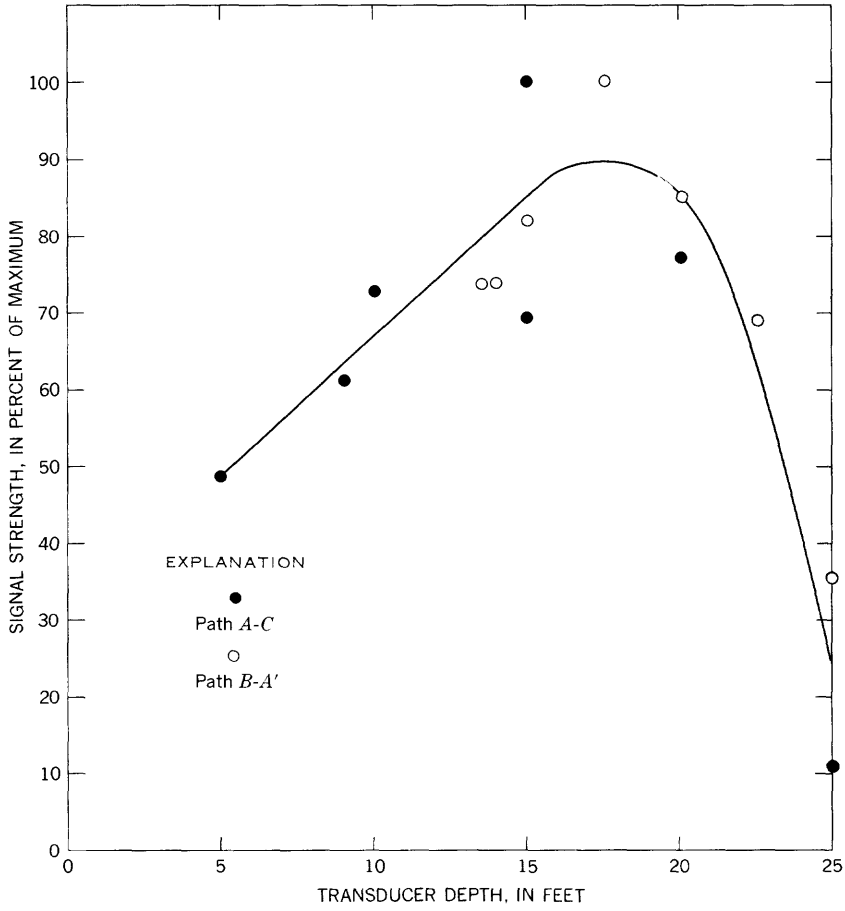

FIGURE 17.—Relation between signal strength and depth of acoustic path.

later in the present report, are also plotted in figure 17. The variation shown confirms trends indicated by previous test work at the Tracy installation. The maximum received signal strength occurs when the acoustic path is well separated from the water surface or the channel bottom. Significant decrease in signal strength occurs as the path nears the water surface; as the path approaches the bottom, signal transmission capability is nearly lost. The tests showed that excellent signal transmission could be achieved along either path *A–C* or path *B–A'* at depths ranging from about 10 to 22 feet.

The loss of signal strength for acoustic paths close to the channel bottom is demonstrated in figure 18, where relative signal strength is plotted against the minimum distance between the path elevation and the channel bottom. The abscissa chosen in figure 18 runs in the reverse

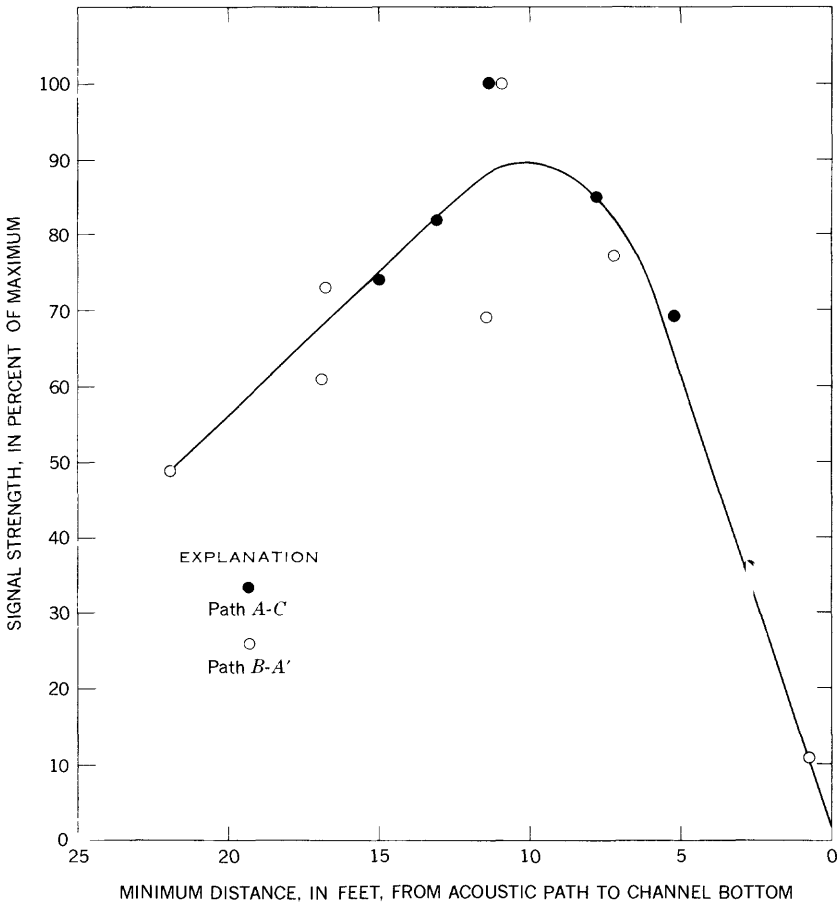

FIGURE 18.—Relation between signal strength and distance from acoustic path to channel bottom.

direction so that figures 17 and 18 can be compared directly.

As the velocity increased from slack tide to ebbtide, difficulty was encountered during the test work on path *A–C* because of extraneous noise in the receiving equipment. The hydrophones were mounted above 50-pound sounding weights suspended on ⅛-inch cable. The "singing" of this cable at appreciable velocities and depths was picked up by the hydrophones and masked the signal being transmitted. Some improvement resulted when the sounding lines were replaced with heavy manila rope, and the test program on this path was completed. Velocities in the channel at point *B* tend to be higher than those at *C*, and when the same setup was used along a path from *A* to *B*, results were too poor for analysis, indicating the need for a more stable hydrophone mount.

No usable structures were in the channel near the *B* position, but there was a substantial pile cluster supporting the Mallard Island channel beacon near *A* (position *A'* in figs. 14 and 15*B*). Because of time limitations, it was not possible to provide a movable hydrophone mount on that pile cluster; therefore, a fixed mount at an elevation of −12.7 feet was installed as an expedient. The barge was moved to position *B*, permitting tests over acoustic paths running from the transducer at variable elevations at *B* to the fixed hydrophone mounted at *A'*. Length of path *B*–*A'* was 3,750 feet. Use of a hydrophone at a fixed elevation at *A'* does not seriously compromise the data, because the channel is deep there, and lowering of the hydrophone would not have placed the acoustic path significantly closer to the channel bottom. Acoustic paths running over the shallow bench extending into the channel from the north shore were similar to those along path *A*–*C*. However, it was not possible to test acoustic paths at elevations near the water surface as was done on path *A*–*C*.

Three test programs were executed along path *B*–*A'*. The first was a repetition of the test made on path *A*–*C* to establish a relation between the signal strength and path depth. The second program was a 7-hour test to determine whether significant changes in signal transmission might result from variation in the flow regime. For this test the transducer elevation was maintained within ±0.3 foot of the hydrophone elevation, and signal transmissions were made at 15-minute intervals. It was thought that signal strength might be affected by stream velocity, so velocity observations were simultaneously recorded with Price current meters at *B* and *A'* for such a comparison.

Data from this program, plotted in figure 19, are not considered conclusive. There was a variation of 45 percent between the maximum and minimum recorded signal strength during the test period, which ran from early in the floodtide period to the slack-water period February 2. The cause for the variation is not known. It may have been associated with changes in the flow regime, changes in sediment concentration, changes in transducer orientation, or drift in the recording equipment, which was powered by a portable generator of unknown voltage stability. Changes of the magnitude recorded would significantly affect calibration of an AVM of the USGS design. It was not economically possible to explore this phase of the problem in greater detail to determine the particular causes involved. However, the test program did demonstrate that signal strength variations will occur and that an AVM designed for use in this channel must be capable of accommodating such changes.

The third test program conducted along path *B*–*A'* was the determination of the beam width of the acoustic signal produced by the

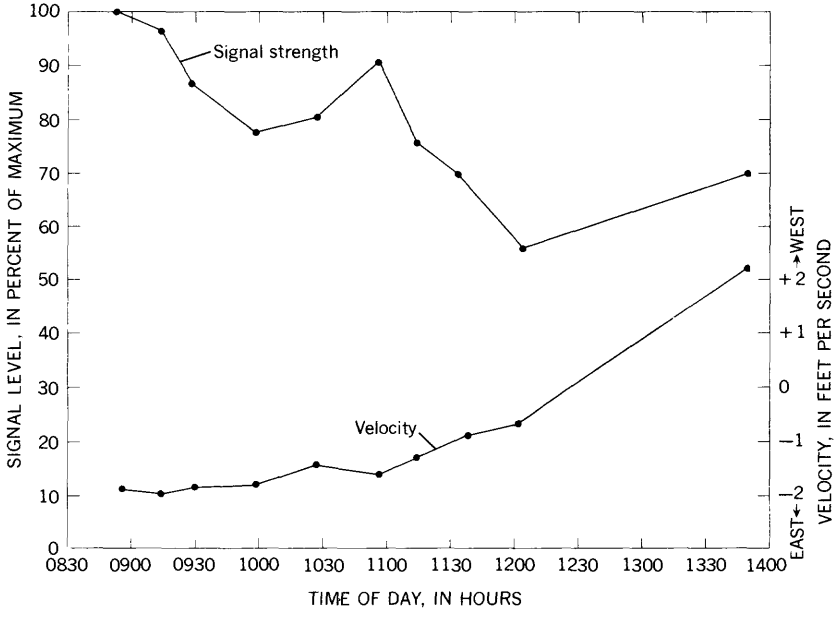

FIGURE 19.—Variation in signal strength with time.

transducers employed in the USGS system. Tests conducted in a small tank and at the Tracy, Calif., site indicated a relatively narrow sound beam with a significant decrease in signal strength as the receiving hydrophone was moved away from the axial line of the transducer. Neither of these tests duplicate exactly the conditions of an open channel because of the proximity of boundaries—the tank walls in the laboratory experiment and the concrete canal lining at the Tracy site—which may conceivably reflect part of the acoustic signal.

If a two-path system were employed for an installation at Chipps Island, a single fixed transducer at the apex of the two paths would be desirable. This would be possible if the beam width of the transducer were broad enough to produce satisfactory signals along paths at angles up to $\pm 45°$ from the axis of orientation.

Measurement of the acoustic beam width can be made by the simple procedure of varying the alinement between the transducer face and the receiving hydrophone and determining the relative signal strength as a function of the angle between the acoustic path and the normal to the transducer face. This was the procedure used in the tests at Tracy, in the test tank, and in the field at Chipps Island. Data from the Chipps Island observations and from the Tracy site are shown on the polar-coordinate plot in figure 20. These data show that the acoustic

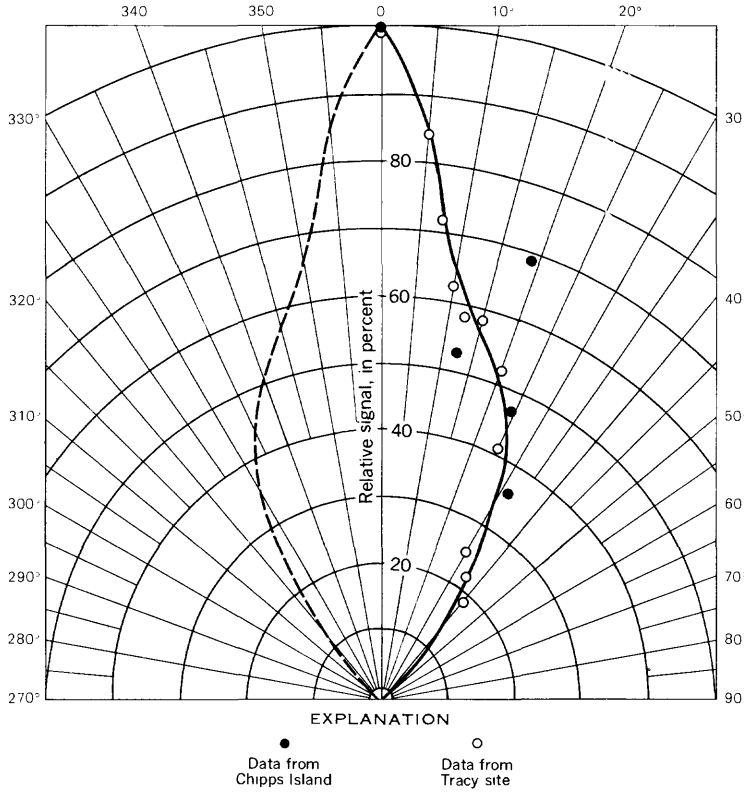

FIGURE 20.—Polar coordinate plot showing acoustic beam width of U.S. Geological Survey transducer.

beam produced by the transducer is moderately narrow. A 15-percent reduction in signal strength occurs within +5° of the axial orientation, and characteristics of the acoustic wave front also change as the departure from the normal increases.

These studies show that careful alinement must be maintained between the transucer and the acoustic path; hence, separate transducers, one for each acoustic path, will be required at the apex of the proposed two-path system.

TWO-PATH SYSTEM

Analysis of the channel hydraulics indicated the need for a two-path metering system to minimize the effects of variations in streamline orientation. Study of the mathematical relations involved in application of such a two-path system also indicated that the timing

errors of the USGS instrument could be determined by comparison of the acoustic propagation rate (c) computed for each leg of such a system. If the temperature and salinity were the same for both paths, then the values of c, computed for each path from equation 16, should be identical. Any difference in computed c values would indicate errors in timing, and the equations developed showed that the errors could be evaluated if certain assumptions proved valid.

Verification of this concept would permit continuous check to be made of instrumental stability, virtually eliminating questions as to instrumental error. A prototype installation was therefore made at the test site on the Delta-Mendota Canal near Tracy, Calif., to permit this verification. The configuration of this prototype system followed the general pattern shown in figure 11. Path lengths were about 300 feet, and the angle between the two acoustic paths was 156°. The transducer at the apex of the system was supported on a motor-driven rotating mount. The unit was programed to squentially record data from the two paths within an interval of 30 seconds. The underwater structures were installed during the period December 1965–January 1966, when the canal was dewatered. Modifications of the console and control equipment were completed during February, and a series of four test runs was made in March 1966. Initial tests were made with balanced signal levels from each transducer. In each of the three subsequent runs the signal strength from one of the transducers in the system was lowered while the other two were held at full power. Power level was first reduced at the central transducer, which was common to both legs of the system, then the power level was restored at this point and successively reduced at the far ends of the two legs. If the assumptions made in the mathematical model of this two-path system were valid, calibration changes resulting from changes in relative signal level could be determined and corrected for by manipulation of the output data.

Results from the test program were disappointing. The first test run showed that the system could be carefully adjusted to produce equivalent results from the two paths, but when the relative signal levels were reduced, it was not possible to manipulate the data to determine the magnitude or the direction of errors introduced. This implies that one or more of the assumptions made in the mathematical model were invalid and that the hoped for instrumental stability cannot be achieved for the USGS system by use of a two-path system. Such a system would permit determination of periods when the data were correct, but it would not provide the data necessary to correct periods when errors were indicated.

CONCLUSIONS REACHED FROM FIELD-TEST PROGRAMS

The following conclusions can be made on the basis of the field tests conducted in the Chipps Island channel and at the Delta-Mendota test site:

1. Acoustic signals of suitable quality could be transmitted over the required distances and at the desired elevations in the Chipps Island channel.
2. Gradual variations of signal strength of the magnitude registered during a 7-hour test period would cause calibration problems with the USGS system.
3. The beam width of the acoustic signal produced by the USGS transducer is moderately narrow. Alinement should be maintained within $\pm 3°$ for proper performance.
4. Instrumental calibration errors of the USGS system cannot be evaluated by manipulation of data from a two-path system. In consequence, it follows that this system cannot be used for measuring the outflow in the Chipps Island channel. Its small systematic error characteristics would introduce gross errors into figures of computed net outflow, and there is no objective method available for determining the magnitude or direction of the errors involved.

ANALYSIS OF ERROR IN COMPUTED DISCHARGE OBTAINED WITH AN IDEAL ACOUSTIC-VELOCITY-METER SYSTEM

Feasibility of measuring the net outflow from the Sacramento–San Joaquin delta in this tidal reach cannot be ruled out because of the limitations of the USGS equipment; research on similar systems has been conducted by private concerns concurrently with the cooperative investigations by the U.S. Geological Survey. Other units are now being marketed, and it is quite possible that some alternate system may prove to have the needed instrumental accuracy. For this reason, an overall statistical evaluation of error sources in an idealized system is desirable. This section of the report summarizes the interrelations among the errors associated with the velocity-index method of flow measurement, the calibration errors stemming from the current-meter measurements required for definition of the hydraulic relations, and the effect of these combined errors on computed values of net outflow.

CALIBRATION TECHNIQUE

Calibration for each path of an AVM in a tidal channel will depend upon an empirical evaluation of the constants in equation 19.

$$Q=\frac{A_p C \tan \theta B}{2}\left[\frac{1}{T_{BA}}-\frac{1}{T_{AB}}\right]$$

For an idealized system this can be written as

$$Q=A_p C \tan\theta\, V_E \tag{24}$$

where

V_E=the velocity recorded by the AVM $\left(\text{equal to } \frac{B}{2}\left[\frac{1}{T_{BA}}-\frac{1}{T_{AB}}\right]\right.$ in the USGS system$\Big)$.

The preceding analysis has dealt with the factors C and θ as separate variables to properly describe the mathematics of the system. However, in the calibration program it will be neither practical nor necessary to evaluate them separately, and they will be treated as a single parameter. Equation 24 will thus reduce to

$$Q=A_p K V_E \tag{25}$$

where $K=C \tan\theta$.

The procedure contemplated for calibration is as follows:

1. The cross-sectional area (A) at the measuring site will be defined by a series of soundings that will define the relation between stage (H) and depth at any point within ± 2 percent. Similar data will be obtained for cross sections along the two acoustic paths (A_{p1} and A_{p2}).
2. An AVM system will be operational, providing readouts of water stage in the channel and of V_E for each of two paths at intervals of 15 minutes or less.
3. Current-meter measurements will be made (by an appropriate method) which will provide velocity readings at points 0.2 and 0.8 of the depth below the water surface at 30 verticals in the cross section once each hour.
4. The measured discharge will be computed by first plotting a curve of discharge versus time for each subarea associated with a vertical; total instantaneous discharge will then be computed on an hourly basis as the sum of discharges in each subsection for the respective time.
5. Data available for calibration will thus include:
   a. Relations of area (A) versus stage (H) for the cross sections along the acoustic paths and for a cross section normal to the channel.
   b. A readout of V_E and stage from the AVM.
   c. The measured discharge (Q_M) at hourly intervals.

6. The coefficient K equal to $C \tan \theta$ for each leg of the AVM system will be computed as

$$K=\frac{Q_M}{A_p(V_E)} \tag{26}$$

where A_p and V_E are derived from the A_p versus H relations and the V_E output for each leg of the system. The mean velocity in the channel will be computed as

$$\overline{V}=\frac{Q_M}{A}$$

7. Correlation between K and $\overline{V}$ will be made by separating data into four periods: Increasing ebbflow, decreasing ebbflow, increasing floodflow, and decreasing floodflow. Plots of K versus $\overline{V}$ similar to figure 7 will then be made for each leg of the system.

COMPUTATION OF NET OUTFLOW

The desired output from the AVM system is a measure of the average net outflow ($\overline{Q}_n$) from the delta area to San Francisco Bay. Because of variations in the large quantity of water stored in the delta channels, $\overline{Q}_n$ will be meaningful only when computed for the 14-day periods between times of equivalent upstream storage. These are periods between nodal points in the lunar cycle. Computations of $\overline{Q}_n$ for other periods will require corrections for changes in upstream storage to be of significance.

Probable errors inherent in the computation of $\overline{Q}_n$ can best be visualized by reference to the formula that will be applied. As $\overline{Q}_n$ is merely the period average of the ebbflows (positive flows) and the floodflows (negative flows) the equation is:

$$\overline{Q}_n=\sum_{i=1}^{N}\left(A_{p_{1_i}}K_{1_i}V_{E_{1_i}}+A_{p_{2_i}}K_{2_i}V_{E_i}\right)/2N \tag{27}$$

where subscripts 1 and 2 refer to the two legs of the AVM system and N is the number of hours or data sets recorded during the cycle under consideration.

Evaluation of A_{p_1} and A_{p_2} would be made from the A versus H relations discussed previously. An iterative routine would be required for evaluation of K_1 and K_2 from curves corresponding to figure 7 because these coefficients are dependent upon the magnitude of $\overline{V}$ and the phase of the tidal cycle.

Error sources to be evaluated are those applicable to the relations of A versus H, relations of K to $\overline{V}$ and tide phase, and the instrumental error in V_E. Errors in the A versus H relations may include a systematic

error of the order of 1 percent and a random error of about 0.2 percent resulting from errors in the stage record. Errors in V_E, for the purpose of the analysis, are assumed to be small and random in character. The significant error source is thus in the relations of K to $\overline{V}$ and tide phase. Errors from this source relate to the random effects of variations in the flow regime in the channel and errors in the discharge measurements used to define the coefficient. To assess the probable error in this relation, an analysis of errors in the discharge measurements is therefore required as a first step.

ACCURACY OF CURRENT-METER MEASUREMENTS

A number of different techniques for measuring the discharge in a tidal reach have been developed by various research teams; common to all is the concept of definition of the relation of subsection discharge versus time at a number of stations across a channel and the computation of instantaneous total discharge as the summation of the incremental discharges. For this analysis the method considered is the so-called moving-boat procedure used by the California Department of Water Resources (formerly called the Water Project Authority of the State of California) in the 1954 investigation. This procedure, described below, seems to be one of the most reliable techniques available.

In the 1954 moving-boat measurement, buoys were placed in the channel to mark the measuring stations as shown in figure 21. Transits were placed on the range lines established at points 1 and 2, and current-meter equipment was mounted on a suitable tugboat. The course of the boat followed the line shown in figure 21. Measurement of velocities was made simultaneously at the 0.2- and 0.8-depth points; depths were determined from curves or tables relating depth at each station to stage. The velocity of the boat (only enough to maintain steerageway) was determined by stopwatch measurement of the transit time of the boat between the established range lines. Water velocity was computed as the difference between the recorded current-meter velocities and the computed boat velocity.

Carter and Anderson (1963) described a statistical technique for analysis of discharge-measurement error. Considered in their treatment were the combined effects of instrument errors, errors due to velocity pulsation, errors due to variation in the velocity distribution in the vertical, and errors related to the number of subsections taken in a measurement. Additional error sources must be included for a tidal-cycle measurement. These additional errors are related to repetitive positioning of the boat in a given subsection, measurement of the boat velocity, variation in the angle of streamflow relative to the cross section, errors in the depth, and errors in the recorded velocities

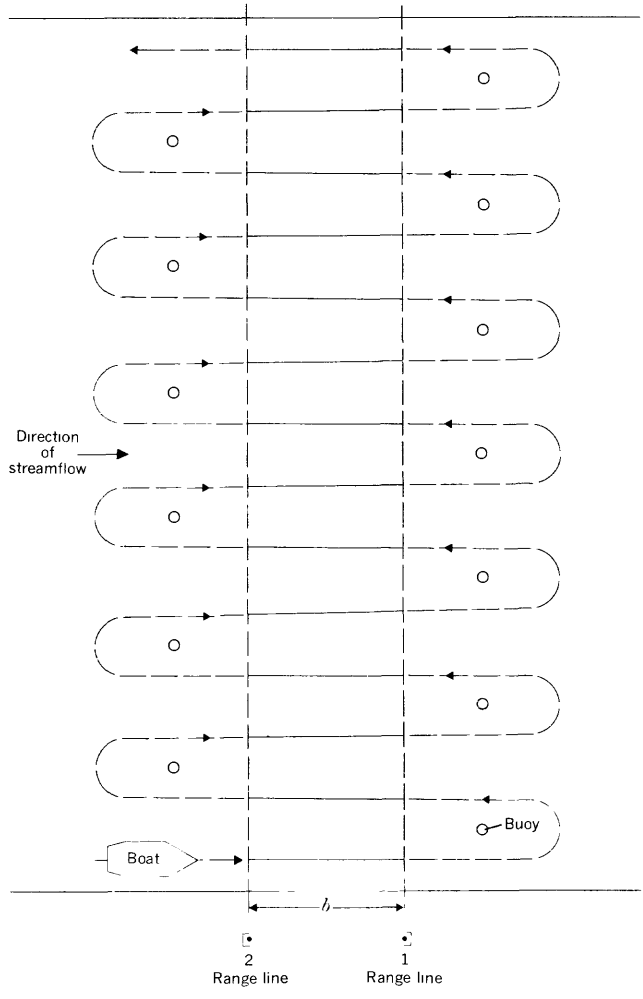

FIGURE 21.—Procedure used in the moving-boat method of streamflow measurement.

resulting from vertical motion of the boat in response to waves in the channel.

Errors introduced by the number of sections employed in the measurement will apply to the total measured discharge, as will errors due to current-meter ratings. Other error sources noted apply to the subsection discharges. Analysis is therefore directed first to evaluation of errors in the computation of subsection discharge (q) and the development of curves of q versus time.

ERRORS IN COMPUTATION OF SUBSECTION DISCHARGE

Statistical concepts and definitions used are summarized in table 8.

Each value of the partial error ratio (r) in table 8 is the error in discharge attributed to the specific source expressed as a percentage of the true discharge; for example, r_t is the partial error ratio attributed to the pulsations in the velocity. The standard deviation (S) of a ratio (r) is a measure of the distribution of the particular error ratio. S_{r_q}, the standard deviation of the subsection discharge error (r_q) may be obtained from:

$$S_{r_q}^2 = S_{r_t}^2 + S_{r_s}^2 + S_{r_l}^2 + S_{r_p}^2 + S_{r_b}^2 + S_{r_a}^2 + S^2_{r_{vb}} \tag{28}$$

Values for the probable standard deviations of error sources 1 and 2 in table 8 are those reported by Carter and Anderson (1963). Values assigned to error sources 3–7 were estimated as described below.

Determination of the angle of streamflow relative to the cross section should be practical within $\pm 3°$, and errors in this measurement can be assumed to be randomly distributed. An error of $\pm 3°$ is equivalent to ± 0.2 percent; therefore, the standard deviation of r_1 is estimated to be 0.2 percent.

TABLE 8.—*Statistics of principal sources of error in subsection discharges*

Source of error	Partial error ratio	Standard deviation of ratios	Probable value of standard deviation in percentage of true q
1. Velocity pulsation	$r_t = \frac{q - q_t}{q}(100)$	S_{rt}	4.2
2. Variation of shape of vertical velocity curve.	$r_s = \frac{q - q_s}{q}(100)$	S_{rs}	[1] 6.3
3. Horizontal angle	$r_l = \frac{q - q_l}{q}(100)$	S_{rl}	.2
4. Boat position	$r_p = \frac{q - q_p}{q}(100)$	S_{rp}	1.2
5. Boat velocity	$= r_b \frac{q - q_b}{q}(100)$	S_{rb}	1.
6. Subsection area	$r_a = \frac{q - q_a}{q}(100)$	S_{ra}	.1
7. Vertical boat velocity	$r_{vb} = \frac{q - q_{vb}}{q}(100)$	S_{rvb}	0

[1] Corrected for correlation between adjacent sections assuming 30 sections used in measurement.

Analysis of the velocity distribution in the Chipps Island channel shows that the average change in velocity per foot of horizontal movement is 0.06 percent of the mean cross-section velocity. For the technique employed in the moving-boat procedure, lateral errors in boat position on repetitive observations in a given subsection can be expected to be of the order of ± 20 feet. Lateral departures of this magnitude may therefore introduce a corresponding error in the velocity of ± 1.2 percent, the value assigned to S_{r_p}.

Assessment of the magnitude of probable error resulting from erroneous evaluation of boat velocity was made as follows (refer to fig. 21):

1. Assume the range distance, b, to be 300 feet.
2. Assume the boat velocity relative to the water, v'_b, to be 5 fps.
3. Assume the water velocity, v, to be 1.5 fps.
4. Assume accuracy of timing of the boat travel from range line 1 to range line 2 to be ± 0.2 second.

The traveltime for boat movement from range line 2 to range line 1 in the downstream direction (T_D) should be

$$T_D = \frac{b}{v'_b + v} = \frac{300}{5+1.5} = 46.2 \text{ seconds;}$$

and the traveltime for boat movement from range line 1 to range line 2 in the upstream direction (T_U) should be

$$T_U = \frac{b}{v'_b - v} = \frac{300}{5-1.5} = 85.8 \text{ seconds.}$$

An error of ± 0.2 second in the measurement of T_D will be reflected by an error of $0.2/46.2 = \pm 0.43$ percent of the value of $(v'_b + v)$, which is equivalent to an error of ± 0.028 fps. This is the error which will be introduced into the computed value of v. In the measurement of Tv, a similar timing error of ± 0.2 second will result in an error in v of ± 0.008 fps. The average of these, ± 0.018 fps, is equivalent to an error of ± 1.2 percent for the velocity of 1.5 fps used in this example. The assumptions made in this calculation are considered typical of the problem, and the error value of 1.2 percent is considered a reasonable approximation for S_{r_b}.

Errors in the subsection area (a) will include a systematic error related to the accuracy of definition of the standard cross section and a random error resulting from errors in the recording of stage. Effects of the random-error component are of primary concern in the computation of the subsection discharges; significance of the systematic-error component will be discussed later. Magnitude of the random error in the subsection area will be controlled by the precision of the stage record obtained.

Instantaneous errors in this record, resulting from the combined effects of wave action, wind, and lag of the stage recording system during periods of rapidly changing stage, should be no more than ± 0.05 foot. The average depth in the channel is about 35 feet; thus, an error of ± 0.05 foot will be equivalent to ± 0.1 percent, the value assigned to S_{r_a}.

Current meters, such as the Price or the Ott, tend to yield erroneous readouts when subject to vertical motion. Work done by Kallio (1966) evaluated the effects of vertical motion of various amplitudes and frequencies and yielded some insight into the registration errors of these instruments under conditions likely to be encountered in a channel such as the one under consideration. Tables 9 and 10, which are taken from the report by Kallio (1966), show, respectively, the registration errors for the Price and Ott-Cosine current meters as related to vertical motion and stream velocity. These data show that the error expressed as $S_{r_{vb}}$ can be virtually eliminated if the Ott current meter is used and if the vertical motion of the meter is held to less than 0.6 fps. These conditions can be met by using a boat of several tons displacement, such as a tugboat, and by avoiding operations during extreme weather conditions.

TABLE 9.—*Tabulation of registration errors, in percentage of stream velocity, for the Price current meter suspended by a cable*

Stream velocity (fps)	Registration error, in percentage of stream velocity, for indicated rates of vertical motion in feet per second, of the current meter						
	0.2	0.4	0.6	0.8	1.0	1.2	1.5
0.5	−2.0	+10	+36	+72	+120	+150	+210
1.0	−3.0	−1.0	+10	+24	+40	+50	+56
1.5	−6.7	−6.7	−4.0	+1.3	+8.0	+15	+27
2.0	−2.5	−2.5	−2.5	−2.0	0	+4 0	+14.0
2.5	0	0	0	0	0	+.8	+4.0
3.0	0	0	0	0	−2.3	−2.0	0
4.0	0	0	0	0	−1.3	−1 3	0
5.0	+.4	+1.0	+.6	0	−.2	0	+.8
7.0	−.7	−.4	0	−.1	−.4	−.7	−.4
10.0	−.5	−.3	0	0	−.3	−.7	−1.3

TABLE 10.—*Tabulation of registration errors, in percentage of stream velocity, for the Ott current meter with Cosine rotor 8646A, standard tailpiece without vertical stabilizer, and two-pin attachment to cable hanger*

Stream velocity (fps)	Registration error, in percentage of stream velocity, for indicated rates of vertical motion in feet per second, of the current meter						
	0.2	0.4	0.6	0.8	1.0	1.2	1.5
0.5	0	+6.0	+10	+20	+30	+44	+70
1.0	0	0	0	+4.0	+9.0	+15	+30
1.5	0	0	0	+1.3	+4.0	+7.3	+17
2.0	0	0	0	+.5	+2.0	+4 5	+9.5
2.5	0	0	0	0	+1.6	+2.8	+6.4
3.0	0	0	0	+.3	+1.0	+2.3	+6.0
4.0	0	0	+.5	+1.0	+1.8	+2.5	+3.8
5.0	+.4	+.6	+.4	+.6	+1.0	+1.4	+2.0
7.0	0	0	0	0	+.3	+.7	+1.4

Computation of S_{r_q} from the error ratios listed in table 8 and equation 28 yields the following:

$$S_{r_q}{}^2=4.2^2+6.3^2+0.2^2+1.2^2+1.2^2+0.1^2+0^2$$

$$S_{r_q}=\sqrt{60.26}=7.8 \text{ percent.}$$

ERRORS IN COMPUTATION OF TOTAL MEASURED DISCHARGE

Error ratios involved in the computation of total measured discharge are listed in table 11. These include the random errors in current-meter calibration, the previously evaluated random errors in the measurement of subsection discharges, the random errors related to the horizontal distribution of flow which are regulated in large part by the number of subsections used in the total measurement, and the systematic errors introduced by the use of a standard cross section. The standard deviation of each of the random error ratios can be evaluated as discussed below, and these can be combined by a truncated version of equation 28 to give a measure of the random error in the total measured discharge. Systematic errors must be added to this random error to estimate the magnitude of the total error.

Analysis of available evidence as to stability and accuracy of current-meter calibration leads to the conclusion that the error ratio (R_{CM}) can be assumed to have a mean of zero and a standard deviation ($S_{R_{CM}}$) of 1 percent if several current meters are used in the measurement program. However, if a single meter was used for all measurements, R_{CM} would not be random, but would appear as a small systematic error applicable equally to both ebbflow and floodflow measurements. It is assumed here that several current meters are used in the measurement program and that R_{CM} is a random variable with a standard deviation of 1.0 percent.

TABLE 11.—*Error ratios and statistical concepts applicable to computation of total measured discharge*

Source of error	Partial error ratios	Standard deviation of ratio	Probable value of standard deviation in percentage of true Q
Current-meter calibration.	$R_{CM}=\frac{Q-Q_i}{Q}(100)$	$S_{R_{CM}}$	1.0
Section discharge	$R_q=\frac{Q-Q_q}{Q}(100)$	$S_{R_q}=\frac{S_{r_q}}{\sqrt{N}}$	1.4
Number of sections	$R_N=\frac{Q-Q_N}{Q}(100)$	$S_{R_N}=f(N)$	1.6
Area definition	$R_a=\frac{Q-Q_a}{Q}(100)$	----------	----------

If it is assumed that a discharge measurement includes N sections of equal subsection discharge (q), then the value of S_{R_q} can be computed from the previously evaluated figure of S_{r_q} by the formula $S_{R_q}=S_{r_q}/\sqrt{N}$. Thus, if 30 subsections are used in the measurement, the standard deviation, S_{R_q}, becomes $S_{r_q}/\sqrt{30}=7.8/\sqrt{30}$, or 1.4 percent.

Data presented by Carter and Anderson (1963) provide an evaluation of S_{R_N} of 1.6 percent for a measurement containing 30 subsections. This statistic, however, applies to the random-sampling error expected for measurements made at separate sites and cannot necessarily be considered a random error applicable to repetitive measurements made at a given site. If the same stationing were used each time, errors from this source—that is, the number and position of verticals selected in the cross section—would probably be systematic and of different magnitude for flood and ebb flows. To reduce S_{R_N} to a value as low as 1.6 percent in this application, the development of a measuring routine which avoids repititious use of the same stationing and number of verticals in successive measurements will be required.

Definition of the cross-sectional area and development of the area versus stage relations for the measuring section can probably be achieved with a precision of ± 1 percent. Errors made in the area versus stage relation will enter subsequent computations as a systematic error, applicable equally to flood and ebb discharges and also to net flow computations.

Random-error sources in the computed total instantaneous discharges will thus include those resulting from R_{c_M}, R_q, and R_N; added to these random-error sources will be systematic error in R_a. Thus, computed values of instantaneous discharge may have a constant error of as much as 1 percent and a random error with a standard deviation $S_{R_M}=(S_{R_{CM}}{}^2+S_{R_q}{}^2+S_{R_N}{}^2)^{1/2}$ of ± 2.4 percent.

ERRORS IN NET OUTFLOW COMPUTATIONS BASED ON CURRENT-METER MEASUREMENTS

Computations of net outflow, based on hourly current-meter measurements, will be affected by the combined errors in the algebraic summations of total ebbflow and floodflow volumes over the period selected. The average net outflow can be expressed as

$$\overline{Q}_n=\sum_1^N Q_M/N \tag{29}$$

Error terms associated are of two types as discussed above. The magnitude of the systematic error (ϵ_A) is equal to

$$\overline{Q}_n(R_a)\cong 0.01\ \overline{Q}_n \tag{30}$$

The standard deviation of the random error (S_N) depends upon N, the number of hourly measurements included in the average, and the average gross flow during the period. This can be expressed as

$$S_N=\left(\frac{S_{R_M}}{\sqrt{N}}\right)\left(\sum_1^N |Q_M|\right)\Big/N, \tag{31}$$

where S_{R_M} is equal to 0.024 for a measurement of the quality considered here. Evaluation of these errors for typical flow rates and observation periods is given in table 12.

TABLE 12.—*Probable errors in net outflow computations based on current-meter measurements*

Average discharge (cfs)			Probable error in measured net outflow (cfs)[1]			
Ebbflow	Floodflow	Net outflow	ϵ_A	S_{24}	S_{72}	S_{336}
150, 000	−148, 000	2, 000	20	±730	±420	±190
150, 000	−147, 000	3, 000	30	±730	±420	±190
150, 000	−146, 000	4, 000	40	±730	±410	±190
150, 000	−145, 000	5, 000	50	±730	±410	±190

[1] ϵ_A is systematic error in area table $\cong$ [1 percent]. S_{24}, S_{72}, S_{336} are the standard deviations of random errors in means computed for periods of 24, 72, and 336 hours, respectively.

COMBINED EFFECT OF CURRENT-METER MEASUREMENT ERRORS AND CALIBRATION ERRORS IN AN ACOUSTIC-VELOCITY-METER SYSTEM

Determination of the relation of K versus velocity and tide phase by application of the equation $K=Q_M/[A_PV_E]$ will result in the inclusion of errors from all sources in the coefficient K. However, errors introduced by the area (A_P) and V_E factors will be compensated for in subsequent application of equation 27 as long as the channel geometry remains unchanged and no drift in instrument accuracy occurs. Thus, the significant error sources are those in the current-meter measurements and those in the relation between the line velocity and the mean velocity in the cross section.

Previous analysis has shown that C (equivalent functionally to K) had a standard deviation of 2.6 percent as derived from 108 computations based on the 1954 measurement data. Part of this scatter may be due to measurement errors, but there is no way of separating the error sources in the analysis applied. It is therefore necessary to assume that a random variation of this magnitude may exist in the relation between line velocities and the mean velocity in the cross section. If these errors and the errors in the current-meter measure-

ments are considered independent, then an approximate value for S_K, standard deviation of K, can be computed as

$$S_K=\sqrt{S_C{}^2+S_{R_M}{}^2}=\sqrt{2.6^2+2.4^2}=3.5 \text{ percent}$$

for each path and, for a two-path system,

$$S_K=3.5/\sqrt{2}=\pm 2.5 \text{ percent.}$$

This value of S_K would represent the anticipated scatter of computed values of K about a curve similar to that developed in figure 7. The question then arises as to the standard error of estimate applicable to such a curve. If the curve were developed analytically by use of techniques applicable to cyclic data, such as the moving-arc method or the method of double integration (Langbein, 1960, p. 59–65), a theoretical evaluation of the standard error of estimate could be made; however, this is not warranted with the data available. A conservative estimate for the accuracy of the curve is that its standard error of estimate is no less than S_K and that systematic errors, related to the cross-sectional area in the measuring section, would be additive. Thus, the overall error in gross discharges computed from a two-path AVM system may include a systematic area-component error of about 1 percent, applicable to both ebb and flood flows, plus a random error represented by S_K equal to about 2.5 percent. This error estimate assumes no changes in streamline orientation other than the small random variations occurring during the calibration period, the results of which would be included in the coefficient K, and no changes in channel geometry or instrumental stability of the AVM subsequent to the calibration period.

Consideration must be given at this point to the question of how many instantaneous discharge figures can be legitimately computed from an array of data such as that which would be accumulated in a tidal-cycle measurement of the type considered here. If the curves of discharge versus time for each subsection were produced by an analytic procedure, the standard error of estimate of each curve could be derived. It would follow that an infinite number of instantaneous total discharges could conceivably be computed, reducing the random error in mean discharge figures to almost zero. This procedure is not considered valid; computations at an interval of less than an hour, the frequency at which current-meter velocities were recorded, must be considered as interpolated values which cannot be treated as statistically independent in determination of means over a period. Because of this, the number of K values which can be legitimately computed during the calibration period will be limited to a frequency of about

once each hour, even though the readout from the AVM system may be at a much higher rate. Values of V_E could be computed as the average of many readouts during each hour of the calibration period to reduce the variance resulting from instrument calibration flutter, but the statistically significant number of computed K values is restricted by the need to correspond with independent current-meter data. The implication of this argument is that current-meter measurements conducted over extended periods of time—for example, 5 days or more—will be required to achieve calibration accuracies equivalent to those discussed above.

Following the type of computation used to estimate the error in net outflow based on current-meter measurements, the general magnitude of errors probable from computations based on an AVM system can be estimated as shown in table 13.

TABLE 13.—*Probable errors in net outflow computations based on AVM output*

Average discharge (cfs)			Probable error in computed net outflow (cfs)[1]			
Ebbflow	Floodflow	Net outflow	ϵ_A	S_{24}	S_{72}	S_{336}
150, 000	−148, 000	2, 000	20	±760	±440	±200
150, 000	−147, 000	3, 000	30	±760	±440	±200
150, 000	−146, 000	4, 000	40	±760	±440	±200
150, 000	−145, 000	5, 000	50	±750	±430	±200

[1] ϵ_A is systematic error $\cong$ |1 percent|. S_{24}, S_{72}, and S_{336} are the standard deviations of random errors in average net outflows computed for periods of 24, 72, and 336 hours, respectively.

Results of this error analysis, summarized in tables 12 and 13, should be considered only as demonstrating the general order of magnitude of errors which might occur. The credibility of these figures must be weighed against the probable validity of the many assumptions required in their derivations. A considerable depth of knowledge and experience was brought to bear upon these many assumptions, but areas of subjectivity remain which detract from the confidence which can be placed in the overall analysis.

SUMMARY AND CONCLUSIONS

1. Analysis of available data on the hydraulic characteristics of flow in the Chipps Island channel indicates that a stable relation varying in a definable manner with velocity and tidal phase can be established between an index line velocity and the mean velocity in the cross section.
2. The stability of the relation between an index line velocity and the mean velocity in the cross section is related to the elevation at which the index line velocity is recorded. For the cross section used in this analysis, that of the 1954 measurement program,

computations indicate that maximum stability would be achieved with an acoustic path at an elevation of about 17 feet below the assumed datum. Similar computations based on current-meter measurements defining present flow conditions in the channel will be required for selection of the optimum path elevation for the proposed acoustic-velocity-metering system.

3. An acoustic-velocity-metering system measuring average line velocities along two diagonal paths oriented about 90° from each other will be necessary to accurately compute flows in the Chipps Island channel.
4. Accuracy of computed average net outflow, computed over a 14-day period, can be expected to be in the range of ±250 cfs if the following conditions are met:
   a. An acoustic-velocity-metering system can be procured which has no bias as to direction of flow and for which instrument errors are small and random in character.
   b. A current-meter measuring system capable of duplicating or improving upon results obtained in the 1954 metering program can be developed within the economic limitations that may be imposed.
   c. Calibration measurements, each covering sereval tidal cycles, are made to define any seasonal changes in flow regime. The required frequency of calibration measurements can be determined only on the basis of operating experience.
5. The acoustic-velocity-metering system developed under a cooperative agreement between the U.S. Geological Survey, the California Department of Water Resources, and the U.S. Army Corps of Engineers does not possess the calibration stability required for this application. However, other systems, now in commercial production, may have the desired performance characteristics.

REFERENCES CITED

Baltzer, A. R., and Shen, John, 1961, Computation of homogeneous flows in tidal reaches by finite-difference method, *in* Short papers in the geologic and hydrologic sciences: U.S. Geol. Survey Prof. Paper 424–C, p. C39–C41.

Carter, R. W., and Anderson, I. E., 1963, Accuracy of current meter measurements: Am. Soc. Civil Engineers Proc., Jour. Hydraulics Div., July 1963, p. 105–115.

Craig, F. C., 1963, Variation in velocity distribution in a tide-affected stream, *in* Selected techniques in water resources investigations: U.S. Geol. Survey Water-Supply Paper 1669–Z, p. Z17–Z24.

Chow, V. T., 1959, Open-channel hydraulics: New York, McGraw-Hill Book Co., 680 p.

Dixon, W. J., and Massey, F. J., Jr., 1957, Introduction to statistical analysis: New York, McGraw-Hill Book Co., p. 287–289.

Flammer, G. H., 1962, Ultrasonic measurement of suspended sediment: U.S. Geol. Survey Bull. 1141–A, 48 p.

Kallio, N. A., 1966, Effect of vertical motion on current meters: U.S. Geol. Survey Water-Supply Paper 1869–B, 20 p.

Langbein, W. B., 1960, Fitting curves to cyclic data, *in* Searcy, J. K., and Hardison, C. H., 1960, Double-mass curves: U.S. Geol. Survey Water-Supply Paper 1541–B, p. 59–65.

Miller, E. G., 1962, Observations of tidal flow in the Delaware River: U.S. Geol. Survey Water-Supply Paper 1586–C, 26 p.

Water Project Authority of the State of California, 1955, Report of lunar-cycle measurements of quantity and salinity of outflows from the Sacramento–San Joaquin Delta made September 11–27, 1954: 50 p.

U.S. GOVERNMENT PRINTING OFFICE: 1969 O–334–224